of hepatocytes[40,41]. It also was reported that the average diameters of sinusoidal fenestrae in C57CL/B mice and healthy human are 141 nm and 107 nm, respectively[42]. The average diameter of optimized MENDs was around 80 nm (Fig. 3a), which would permit optimized MENDs to pass through fenestrae and access hepatocytes. Therefore, we assume that MENDs containing YSK05 are taken up by hepatocytes by a process mediated by ApoE-LDL receptor association. This association presumably follows extravasation of MENDs from sinusoidal lumen to Disse through fenestrae, which results in widespread delivery of siRNAs to hepatocytes in healthy and transgenic mice, as well as to human hepatocytes in chimeric mice. The lipid composition for the initial MEND *in vivo* was chosen at YSK05/DSPC/cholesterol/PEG-lipid=50 : 10 : 40 : 3 mol%, as described previously[24,43]. Since DSPC, a helper lipid, was not essential to exert silencing in liver, DSPC was eliminated from lipid envelope (**supplementary** Fig. 2a). The pH-sensitive YSK05 lipid is presumed to be responsible for the endosomal release of the MEND cargo. Hence we tested the silencing activity of siRNA-loaded MENDs with increasing ratios of YSK05; activity was maximized at approximately 70 mol% YSK05. Based on our testing, a MEND composed of YSK05, cholesterol, and PEG-lipid at 70 : 30 : 3 was regarded as the optimized version. For systemic siRNA delivery using ionizable LNPs, lipid pKa value was identified as an important parameter, with optimum pKa in the range of 6.2–6.5[44]. In the present study, the pKa values of initial and optimized MENDs were determined as 6.6 and 6.4 respectively, which fell within this optimal pKa range. The endosomal escape of MEND is presumably mediated by membrane fusion. According to hemolysis activity, optimization of MEND improved fusion ability at acidic pH, but did not affect fusion at neutral pH. This optimization contributed to a 10-fold increase in silencing activity, yielding an ED50 of ~0.06 mg/kg in liver. Our results suggested that efficient siRNA delivery depends on the use of lipid-based nano-carriers that provide both optimized pKa and highly fusogenic characteristics. We also successfully delivered anti-miRNA oligonucleotide against miRNA-122 (miR-122) into hepatocytes using optimized YSK05-MEND, which resulted in efficient miR-122 knockdown and reduced plasma cholesterol level[45,46]. Our results permitted us to attempt delivery of dh-siRNAs to HCV-infected liver using the optimized MENDs. Our steady progress with a liver-targeting delivery system should facilitate the development of a safe and effective strategy for targeting HCV in hepatocytes in the near future.

Although our results were conducted in mouse models for HCV pathogenesis, results from these technologies are expected to provide therapeutic potential against infectious HCV *in vivo*, while also providing a new siRNA design tool for targeting viral seqeunces. Despite other obstacles (e.g., off-target effects), RNAi using these technologies provides a new potential therapeutic application that may effectively treat HCV infection.

Methods

Ethics statements. All *in vivo* experiments were approved by the Institutional Animal Care and Use Committee, and protocols for animal experiments were approved by the local ethics committee. The animals received humane care according to guidelines of the National Institutes of Health. Human patients provided informed written consent before sampling (collection of HCV-containing blood samples).

siRNAs. The design of HCV-directed siRNAs has been described previously[26]. Briefly, we designed nine siRNAs that target the 5′-UTR and 3′-UTR of the HCV genome and examined their efficacy in the *in vitro* inhibition of HCV replication. Of these nine siRNAs, the most effective siE was one directed toward nucleotides 323 to 342 of the HCV genome. The sequences for the sense and antisense strands of the siRNA are as follows: siE sense: 5′-GUC UCG UAG ACC GUG CAU CAU U-3′; antisense: 5′-UGA UGC ACG GUC UAC GAG ACU U-3′. siRNAs were generated by annealing equimolar amounts of complementary sense and antisense strands.

Anti-luciferase siRNA (siLuc) (sense: 5′-CCG UCG UAU UCG UGA GCA ATT-3′; antisense: 5′-UUG CUC ACG AAU ACG ACG GTT-3′) was purchased from Sigma (Ishikari, Japan). Anti-FVII siRNA (siFVII) (sense: 5′-GGAucAucucAA-GucuuAcT*T-3′; antisense: 5′-GuAAGAcuuGAGAuGAuccT*T-3′; lower case letters indicate 2′-fluoro-modified nucleotides, asterisks indicate phosphorothioate linkages) were purchased from Hokkaido System Science Co., Ltd. (Sapporo, Japan).

Dicer-generated siRNAs. We generated the HCV-specific long dsRNA template for *in vitro* transcription by PCR-amplified DNA templates and synthesized Dicer-generated siRNAs (d-siRNAs) by cleavage with recombinant human Dicer (rhDicer; Gene Therapy Systems, San Diego, CA)[26]. By comparison with the silencing efficiency of d-siRNAs, d-siD5-50 and d-siD5-197 silenced the HCV replication more efficiently than synthetic siE (Supplementary information Fig. 1). The template dsRNAs of d-siD5-50 and d-siD5-197 were located at nucleotides 309–358 and 199-395 of HCR6 sequence (GenBank accession number AY045702).

siRNAs predicted by the commercial software. The siRNA design algorithms for antiviral RNAi, siVirus, siDirect and Block-iT (Invitrogen), were used for the selection of the target sequence for siRNA within the specified target HCV genome (nucleotides 199–395).

Cell culture and HCV-replicon assay. We used four HCV subgenomic replicon cell lines, FLR3-1 (genotype 1b, Con-1)[47], R6FLR-N (genotype 1b, strain N)[26], JFH-1/FLR/K4 (genotype 2a)[48], and RMT-tri (genotype 1a)[49], which have the firefly luciferase gene for the sensitive and precise quantification of the HCV replication levels using a luciferase assay. We also used REF cells[30] which harbor the divided-full genome replicon for analysis of the HCV 5′ UTR sequences. Each cell line was seeded at a density of 5×10^3 per well in 96-well tissue culture plates, and grown (at 37°C and 5% CO_2) in complete Dulbecco's modified Eagle's medium supplemented with Glutamax I (Invitrogen, Carlsbad, CA) and containing 5% fetal calf serum (Invitrogen). Cells were transfected with 30 nM siRNA using RNAiMax (Invitrogen, Carlsbad, CA). After 72 hours, luciferase activity was determined in triplicate using the Steady-Glo or Bright-Glo luciferase assay kit (Promega Madison, WI). The luciferase signal was measured using an LB940 luminometer (Berthold, Freiburg, Germany) and the results were expressed as the mean percentage of control. IC_{50} values of siRNA were calculated by nonlinear curve-fitting using the equation: $Y=100-(Y_{Bottom} \times X/(IC_{50} + X))$, where Y represents percent inhibition and X represents the concentration of siRNAs.

5′-rapid amplification of cDNA ends (RACE) analysis. Replicon cells were transfected with synthetic HCV-specific siRNA (siE) and Dicer-generated siRNAs using Lipofectamine RNAiMAX or Lipofectamine 2000 (Invitrogen) according to the manufacturer's protocol. At 6 h post-transfection, total RNA from replicon cells was extracted using the acid guanidinium-phenol-chloroform method[26].

For the RNA oligo ligation method, 5 μg of total RNA was ligated to the GeneRacer RNA adapter (Invitrogen, 5′-CGA CUG GAG CAC GAG GAC ACU GAC AUG GAC UGA AGG AGU AGA AA-3′) without any prior processing. Ligated RNA was reverse transcribed into cDNA using the HCV-specific reverse primer (R6 876-R20 reverse primer: 5′- AGA GGA AGA TAG AGA AAG AG-3′). To detect cleavage product, semi-nested-PCR was performed as follows: first-run PCR used a primer complementary to the RNA adapter (GeneRacer 5′ Nested Primer: 5′-GGA CAC TGA CAT GGA CTG AAG GAG TA-3′) in combination with an HCV-specific primer (R6 610-R24 reverse primer: 5′-CCC TCG TTG CCA TAG AGG GGC CAA-3′); second-run PCR used the same oligo specific primer (GeneRacer 5′ Nested Primer) in combination with a second HCV-specific primer (R6 536-R20 reverse primer: 5′-GAT AGG TTG TCG CCT TCC AC-3′).

For the C-tailing at the 3′-end of RNA method, first-strand cDNA synthesis was performed by using SuperScript II reverse transcriptase (Promega Corporation, Madison, WI) to transcribe total RNA (5 μg) with the HCV-specific reverse primer (R6 876-R20 reverse primer) according to the manufacturer's protocol. The resulting first-strand cDNA was subjected to another round of 5′-RACE using a distinct RACE kit (Cat. 18374-058, Invitrogen, Carlsbad, CA). The first-strand cDNA was tailed at the 3′-end by terminal transferase TdT and dCTP. The primer set consisted of an HCV-specific reverse primer (R6 610-R24) and the Abridged Anchor Primer for the first-run PCR, and an HCV-specific reverse primer (R6 536-R20) and the Abridged Universal Amplification Primer for the second-run PCR.

Amplification fragments obtained by the two independent 5′-RACE methods were resolved on 3.0% agarose and sized using a 1-kb Plus DNA Ladder (Invitrogen). Specific cleavage sites were further confirmed by DNA sequencing.

Dicer-hunting siRNA sequences design. Based on the cleavage site defined by d-siRNAs, reverse genetic approach was applied to the design of Dicer favourable siRNA sequence. A dh-siRNA consists of duplexes of 21-nt RNAs that are base-paired with 2-nt 3′ overhangs.

Preparation of MENDs. Cholesterol, 1,2-distearoyl-sn-3-phosphatidylcholine (DSPC), 1,2-dimyristoyl-sn-glycerol, and methoxyethyleneglycol 2000 ether (PEG-DMG) were purchased from Avanti Polar Lipid (Albaster, AL). The synthesis of YSK05 was performed as previously described[21]. MENDs encapsulating siRNAs were prepared by a *t*-BuOH dilution procedure. Lipid in 90% (v/v) *t*-BuOH was mixed with siRNA in 20 mM citrate buffer (pH 4.0) at siRNA/lipid ratio of 0.1 (wt/wt) under strong agitation to yield a final *t*-BuOH concentration of 60% (v/v). Then, the lipid/siRNA mixture was added into 20 mM citrate buffer (pH 4.0) under strong agitation to yield a final *t*-BuOH concentration of <12% (v/v). Ultrafiltration was performed to remove *t*-BuOH, replacing external buffer with phosphate-buffered saline (PBS, pH7.4) and concentrating the MENDs. A lipid envelope of initial MEND was

prepared using YSK05, DSPC, cholesterol, and PEG-DMG at a molar ratio of 50 : 10 : 40 : 3 as described previously[24,43], and optimized MEND was prepared using YSK05, cholesterol, and PEG-DMG at a molar ratio of 70 : 30 : 3.

Characterization of MEND. The average diameter and zeta-potential of MENDs were determined using a Zetasizer Nano ZS ZEN3600 (MALVERN Instrument, Worcestershire, UK). siRNA encapsulation efficiency was determined by a RiboGreen assay (Invitrogen Carlsbad, CA). MENDs were diluted in 10 mM HEPES buffer (pH 7.4) containing 20 μg/mL dextran sulfate and Ribogreen in the presence or absence of 0.1% (w/v) Triton X-100. Fluorescence was measured by Varioskan Flash (Thermo scientific) with λex=500 nm, λem=525 nm. siRNA concentration was calculated based on a siRNA standard curve. siRNA encapsulation efficiency was calculated by comparing siRNA concentration in the presence and absence of Triton X-100. The pKa of YSK05 in each MEND was determined using 6-(p-Toluidino)-2-naphthalenesulfonic acid (TNS). Thirty μM of MEND lipid and 6 μM of TNS were mixed in 200 μL of 20 mM citrate buffer, 20 mM sodium phosphate buffer, or 20 mM Tris-HCl buffer, containing 130 mM NaCl at a pH ranging from 3.0 to 9.0. Fluorescence was measured by a Varioskan Flash with λex=321 nm, λem=447 nm, at 37°C. The pKa values were measured as the pH giving rise to half-maximal fluorescent intensity.

Hemolysis assay. Fresh red blood cells (RBCs) were collected from ICR mice and suspended in PBS. The RBC suspension was mixed with indicated amount of MEND, incubated at 37°C for 30 min, and then centrifuged (4°C, 400 *g*, 5 min). The absorbance of the supernatant was measured at 545 nm. Positive and negative control samples were prepared by incubation of RBCs with 0.5% (wt/v) Triton X-100 or PBS (respectively). The %hemolysis was epressed as the % of the absorbance of the positive control.

***In vivo* mouse Factor VII knockdown experiments.** Male ICR mice (5–6 weeks old) were purchased from Japan SLC (Shizuoka, Japan). MENDs encapsulating siFVII were diluted to the appropriate concentrations in PBS (pH 7.4) and administered intravenously (IV; via the tail vein) at a dose volume of 10 to 15 mL/kg. At the indicated time points, blood and liver were collected. The blood was processed to plasma, and plasma levels of Factor VII protein were determined using a colorimetric Biophen VII assay kit (Aniara) according to the manufacturer's protocol. The standard curve for Factor VII plasma levels was generated using plasma collected from PBS-treated mice. Total RNA in liver was isolated using TRIzol (Invitrogen) according to the manufacturer's protocol. The resulting RNA was reverse transcribed using a High Capacity RNA-to-cDNA kit (ABI) according to manufacturer's protocol. For each specimen, quantitative PCR analysis was performed on 2 ng of cDNA using Fast SYBR Green Master Mix (ABI) and a Lightcycler480 system II (Roche). All reactions were performed in a volume of 15 μL. The primers for mouse *fvii* were (forward) 5′-TCG AAT CCA TGT CAG AAC GGA GGT -3 and (reverse) 5′-CCG ACC CTC AAA GTC TAG GAG GCA-3′.

***In vivo* microscopic observation.** Optimized MENDs encapsulating Cy5-labeled siRNA were administered into male ICR mice (5–6 weeks old). Five min before projected sacrifice, FITC-conjugated isolectin B4 (40 μg/mouse) was intravenously injected via the tail vein to stain blood vessels. At 30 min after intravenously injection of optimized MEND, each animal was perfused with PBS to remove blood from the liver, then with 4% paraformaldehyde (PFA)-PBS for fixation. Liver tissues were excised and further fixed with 4% PFA-PBS for 24 hr at 4°C, then submerged in 20% sucrose-PBS for 4 hr at 4°C. The liver was embedded in OCT compound (Sakura Fine Technical, Tokyo, Japan) and snap-frozen in liquid nitrogen. Frozen samples were cut in 30 μm-thick sections (LEICA CM3000, Leica Microsystems, Wetzlar, Germany). The samples were stained with Hoechst33342 to detect nuclear DNA, and observed at an excitation wavelength of 633 nm using a laser-equipped Nikon A1 (Nikon Co. Ltd., Tokyo, Japan) with a x60 objective lens.

***In vivo* HCV infection experiments.** We purchased chimeric mice from PhenixBio (Hiroshima, Japan). The chimeric mice were generated by transplanting human primary hepatocytes into severe combined immunodeficient (SCID) mice carrying the urokinase plasminogen activator transgene controlled by an albumin promoter (uPA/SCID)[34]. Six weeks after hepatocyte transplantation, each mouse was injected IV with patient serum containing 10^6 copies of HCV genotype 1b (HCR6; accession number AY045702)[36]. HCV inoculations, drug administration, blood collection, and sacrifice were performed under ether anesthesia. Blood samples were taken from the orbital vein and sera were immediately isolated. Human serum albumin in the blood of chimeric mice was measured with a commercially available kit (Alb-II kit; Eiken Chemical, Tokyo, Japan) and serum ALT level was determined with enzymatic assays (Horiba ABX Diagnostics) according to the manufacturer's instructions[35].

Rhodamine-labeled siRNA was synthesized by Dharmacon (Lafayette, CO). Alexa-546 or Alexa-568 labeled siE/CL-LA was injected IV into BALB/c mice. After 30 minutes, the liver, lung, spleen, and kidney were harvested from each mouse. Sections of these tissues then were stained with DAPI (Molecular Probes) and slides examined using confocal laser microscopy (Zeiss).

Liver tissues obtained from mice were embedded in OCT compound (Ted Pella, Redding, CA). The frozen tissues were cut into thin sections (6 μm) and placed on glass slides. The sections were fixed in 10% buffered formalin and then treated with 0.1% Triton X-100. To detect HCV protein by immunohistochemistry (IHC)[35], the slides were incubated with rabbit anti-core protein IgG and then with donkey anti-rabbit IgG polyclonal antibody (Fab fragment, labeled with HRP; Dako, Glostrup, Denmark). The HRP label was amplified with FITC-conjugated tyramide according to the manufacturer's instructions (Molecular Probes, Eugene, OR). To detect human hepatocytes, liver sections were probed with anti-human hepatocyte monoclonal antibody (Dako), followed by anti-mouse IgG-Alexa 546 (Molecular Probes). Nuclei were stained by DAPI. Normal rabbit IgG was used as a control.

Transgenic mice with persistent HCV protein expression. To provide an immunocompetent model for inhibition of HCV protein expression, a mouse strain harbouring an HCV transgene was generated via a Cre/loxP switching system[37]. We bred CN2-29 transgenic mice, which carry an HCV transgene (nt. 294–3435), with Mx1-Cre transgenic mice, which express Cre recombinase in response to interferon (IFN)-α or a chemical inducer of IFN-α, poly(I:C). Following poly(I:C) injection, the HCV transgene was rearranged, and HCV sequences were expressed in the livers. In this model, HCV structure proteins are expressed in the liver within 7 days after poly(I:C) injection. Male CN2-29 trasgegenic mice (8–9 week-old) were injected intraperitoneally with 0.3 mL of 1 mg/mL poly(I:C) solution [in PBS (-)]. At 6 months after the poly(I:C) injection, the CN2-29 mice were administrated intravenously twice with the siRNA-MEND complex solution [1 mg/mL in PBS(-)] via orbital sinus at day 0 and day 2. The mice were sacrifice under anesthesia with ketamine/xylazine 2 days after the second siRNA-MEND administration. Livers were removed, fixed in 10% buffered formalin, and embedded in paraffin. Section (4 μm) were stained with hematoxylin and eosin, and observed using ZEISS Axio Imager A2 upright microscope (Carl Zeiss MicroImaging, Inc, Germany).

Statistical analysis. The data are expressed as the mean ± S.D. Statistical analysis of the difference between the HCV viral load during treatment and follow-up period and the baseline (day 0) level was conducted using the analysis of variance with a nonparametric Mann-Whitney U test. The probability values $P < 0.05$ were marked with *, and $P < 0.01$ were marked with **.

1. Hoofnagle, J. H. & Seeff, L. B. Peginterferon and ribavirin for chronic hepatitis C. *N Engl J Med* **355**, 2444–2451 (2006).
2. De Francesco, R. & Migliaccio, G. Challenges and successes in developing new therapies for hepatitis C. *Nature* **436**, 953–960 (2005).
3. Gao, M. *et al* Chemical genetics strategy identifies an HCV NS5A inhibitor with a potent clinical effect. *Nature* **465**, 96–100 (2010).
4. Elbashir, S. M., Harborth, J., Lendeckel, W., Yalcin, A., Weber, K. & Tuschl, T. Duplexes of 21-nucleotide RNAs mediate RNA interference in cultured mammalian cells. *Nature* **411**, 494–498 (2001).
5. Hannon, G. J. RNA interference. *Nature* **418**, 244–251 (2002).
6. Reynolds, A., Leake, D., Boese, Q., Scaringe, S., Marshall, W. S. & Khvorova, A. Rational siRNA design for RNA interference. *Nat Biotechnol* **22**, 326–330 (2004).
7. Ui-Tei, K. *et al.* Guidelines for the selection of highly effective siRNA sequences for mammalian and chick RNA interference. *Nucleic acids research* **32**, 936–948 (2004).
8. Patzel, V., Rutz, S., Dietrich, I., Koberle, C., Scheffold, A. & Kaufmann, S. H. Design of siRNAs producing unstructured guide-RNAs results in improved RNA interference efficiency. *Nat Biotechnol* **23**, 1440–1444 (2005).
9. Ameres, S. L., Martinez, J. & Schroeder, R. Molecular basis for target RNA recognition and cleavage by human RISC. *Cell* **130**, 101–112 (2007).
10. Tafer, H. *et al.* The impact of target site accessibility on the design of effective siRNAs. *Nat Biotechnol* **26**, 578–583 (2008).
11. Das, A. T. *et al.* Human immunodeficiency virus type 1 escapes from RNA interference-mediated inhibition. *J Virol* **78**, 2601–2605 (2004).
12. Konishi, M. *et al.* siRNA-resistance in treated HCV replicon cells is correlated with the development of specific HCV mutations. *J Viral Hepat* **13**, 756–761 (2006).
13. Wilson, J. A., Richardson, C. D. & Hepatitis, C. virus replicons escape RNA interference induced by a short interfering RNA directed against the NS5b coding region. *J Virol* **79**, 7050–7058 (2005).
14. Naito, Y., Ui-Tei, K., Nishikawa, T., Takebe, Y. & Saigo, K. siVirus: web-based antiviral siRNA design software for highly divergent viral sequences. *Nucleic acids research* **34**, W448–450 (2006).
15. Westerhout, E. M., Ooms, M., Vink, M., Das, A. T. & Berkhout, B. HIV-1 can escape from RNA interference by evolving an alternative structure in its RNA genome. *Nucleic acids research* **33**, 796–804 (2005).
16. Brown, K. M., Chu, C. Y. & Rana, T. M. Target accessibility dictates the potency of human RISC. *Nat Struct Mol Biol* **12**, 469–470 (2005).
17. Overhoff, M. *et al.* Local RNA target structure influences siRNA efficacy: a systematic global analysis. *J Mol Biol* **348**, 871–881 (2005).
18. Gredell, J. A., Berger, A. K. & Walton, S. P. Impact of target mRNA structure on siRNA silencing efficiency: A large-scale study. *Biotechnol Bioeng* **100**, 744–755 (2008).
19. de Fougerolles, A., Vornlocher, H. P., Maraganore, J. & Lieberman, J. Interfering with disease: a progress report on siRNA-based therapeutics. *Nat Rev Drug Discov* **6**, 443–453 (2007).
20. Kogure, K., Akita, H., Yamada, Y. & Harashima, H. Multifunctional envelope-type nano device (MEND) as a non-viral gene delivery system. *Adv Drug Deliv Rev* **60**, 559–571 (2008).
21. Sato, Y., Hatakeyama, H., Sakurai, Y., Hyodo, M., Akita, H. & Harashima, H. A pH-sensitive cationic lipid facilitates the delivery of liposomal siRNA and gene

silencing activity in vitro and in vivo. *Journal of controlled release: official journal of the Controlled Release Society* **163**, 267–276 (2012).
22. Connor, J., Yatvin, M. B. & Huang, L. pH-sensitive liposomes: acid-induced liposome fusion. *Proc Natl Acad Sci U S A* **81**, 1715–1718 (1984).
23. Straubinger, R. M., Duzgunes, N. & Papahadjopoulos, D. pH-sensitive liposomes mediate cytoplasmic delivery of encapsulated macromolecules. *FEBS Lett* **179**, 148–154 (1985).
24. Semple, S. C. *et al.* Rational design of cationic lipids for siRNA delivery. *Nat Biotechnol* **28**, 172–176 (2010).
25. Tsukiyama-Kohara, K., Iizuka, N., Kohara, M. & Nomoto, A. Internal ribosome entry site within hepatitis C virus RNA. *J Virol* **66**, 1476–1483 (1992).
26. Watanabe, T. *et al.* Intracellular-diced dsRNA has enhanced efficacy for silencing HCV RNA and overcomes variation in the viral genotype. *Gene Ther* **13**, 883–892 (2006).
27. Kim, D. H., Behlke, M. A., Rose, S. D., Chang, M. S., Choi, S. & Rossi, J. J. Synthetic dsRNA Dicer substrates enhance RNAi potency and efficacy. *Nat Biotechnol* **23**, 222–226 (2005).
28. Siolas, D. *et al.* Synthetic shRNAs as potent RNAi triggers. *Nat Biotechnol* **23**, 227–231 (2005).
29. Jinek, M. & Doudna, J. A. A three-dimensional view of the molecular machinery of RNA interference. *Nature* **457**, 405–412 (2009).
30. Arai, M. *et al.* Establishment of infectious HCV virion-producing cells with newly designed full-genome replicon RNA. *Arch Virol* **156**, 295–304 (2011).
31. Pei, Y. & Tuschl, T. On the art of identifying effective and specific siRNAs. *Nat Methods* **3**, 670–676 (2006).
32. Naito, Y., Yoshimura, J., Morishita, S. & Ui-Tei, K. siDirect 2.0: updated software for designing functional siRNA with reduced seed-dependent off-target effect. *BMC Bioinformatics* **10**, 392 (2009).
33. Akinc, A. *et al.* A combinatorial library of lipid-like materials for delivery of RNAi therapeutics. *Nat Biotechnol* **26**, 561–569 (2008).
34. Mercer, D. F. *et al.* Hepatitis C virus replication in mice with chimeric human livers. *Nat Med* **7**, 927–933 (2001).
35. Inoue, K. *et al.* Evaluation of a cyclophilin inhibitor in hepatitis C virus-infected chimeric mice in vivo. *Hepatology* **45**, 921–928 (2007).
36. Tsukiyama-Kohara, K. *et al.* Activation of the CKI-CDK-Rb-E2F pathway in full genome hepatitis C virus-expressing cells. *J Biol Chem* **279**, 14531–14541 (2004).
37. Sekiguchi, S. *et al.* Immunization with a recombinant vaccinia virus that encodes nonstructural proteins of the hepatitis C virus suppresses viral protein levels in mouse liver. *PLoS One* **7**, e51656 (2012).
38. Hutvagner, G. & Simard, M. J. Argonaute proteins: key players in RNA silencing. *Nat Rev Mol Cell Biol* **9**, 22–32 (2008).
39. MacRae, I. J., Ma, E., Zhou, M., Robinson, C. V. & Doudna, J. A. In vitro reconstitution of the human RISC-loading complex. *Proc Natl Acad Sci U S A* **105**, 512–517 (2008).
40. Yan, X. *et al.* The role of apolipoprotein E in the elimination of liposomes from blood by hepatocytes in the mouse. *Biochem Biophys Res Commun* **328**, 57–62 (2005).
41. Akinc, A. *et al.* Targeted delivery of RNAi therapeutics with endogenous and exogenous ligand-based mechanisms. *Mol Ther* **18**, 1357–1364 (2010).
42. Jacobs, F., Wisse, E. & De Geest, B. The role of liver sinusoidal cells in hepatocyte-directed gene transfer. *Am J Pathol* **176**, 14–21 (2010).
43. Sakurai, Yea. Gene Silencing via RNAi and siRNA quantification in Tumor Tissue using MEND, a Liposomal siRNA Delivery System. *Mol Ther* **in press**, (2013).
44. Jayaraman, M. *et al.* Maximizing the potency of siRNA lipid nanoparticles for hepatic gene silencing in vivo. *Angew Chem Int Ed Engl* **51**, 8529–8533 (2012).
45. Takahashi, M. *et al.* In vitro optimization of 2′-OMe-4′-thioribonucleoside-modified anti-microRNA oligonucleotides and its targeting delivery to mouse liver using a liposomal nanoparticle. *Nucleic acids research* **41**, 10659–10667 (2013).
46. Hatakeyama, H. *et al.* The systemic administration of an anti-miRNA oligonucleotide encapsulated pH-sensitive liposome results in reduced level of hepatic microRNA-122 in mice. *Journal of controlled release: official journal of the Controlled Release Society* **173**, 43–50 (2014).
47. Sakamoto, H. *et al.* Host sphingolipid biosynthesis as a target for hepatitis C virus therapy. *Nat Chem Biol* **1**, 333–337 (2005).
48. Wakita, T. *et al.* Production of infectious hepatitis C virus in tissue culture from a cloned viral genome. *Nat Med* **11**, 791–796 (2005).
49. Yasui, F., Sudoh, M., Arai, M. & Kohara, M. Synthetic lipophilic antioxidant BO-653 suppresses HCV replication. *J Med Virol* **85**, 241–249 (2013).
50. Honda, M., Beard, M. R., Ping, L. H. & Lemon, S. M. A phylogenetically conserved stem-loop structure at the 5′ border of the internal ribosome entry site of hepatitis C virus is required for cap-independent viral translation. *J Virol* **73**, 1165–1174 (1999).

Acknowledgments

We are very grateful to Dr. Fumihiko Yasui for his helpful discussion. This work was supported in part by grants from the Ministry of Education, Culture, Sports, Science and Technology (MEXT) of Japan; the Program for Promotion of Fundamental Studies in Health Sciences of Pharmaceuticals and Medical Devices Agency of Japan; the Ministry of Health, Labor and Welfare of Japan; the Special Education and Research Expenses of MEXT of Japan; and a Grant-in-Aid for Scientific Research on Innovative Areas "Nanomedicine Molecular Science" (No. 2306) from MEXT of Japan.

Author contributions

M.K. conceived the study. T.W., H.H., C.M. and Y.S. conducted the study equally. T.W. and H.H. coordinated the analysis and manuscript preparation. M.S. and H.H. had input into the study design and A.T., Y.H. and T.O. accomplished mouse management. M.A. and K.I. revised the manuscript for intellectual content. T.W., H.H., C.M. and Y.S. contributed equally.

Additional information

Supplementary information accompanies this paper at http://www.nature.com/scientificreports

Competing financial interests: Sudoh M. is an employee of Chugai Pharmaceutical Co., Ltd. Arai M. is an employee of Mitsubishi Tanabe Pharma Co., Ltd. The other authors disclose no conflicts.

How to cite this article: Watanabe, T. *et al. In vivo* therapeutic potential of Dicer-hunting siRNAs targeting infectious hepatitis C virus.. *Sci. Rep.* 4, 4750; DOI:10.1038/srep04750 (2014).

OPEN ACCESS Freely available online

PLOS ONE

B-Cell-Intrinsic Hepatitis C Virus Expression Leads to B-Cell-Lymphomagenesis and Induction of NF-κB Signalling

Yuri Kasama[1], Takuo Mizukami[2], Hideki Kusunoki[2], Jan Peveling-Oberhag[3], Yasumasa Nishito[4], Makoto Ozawa[6,7], Michinori Kohara[5], Toshiaki Mizuochi[2], Kyoko Tsukiyama-Kohara[6,7]*

1 Department of Experimental Phylaxiology, Faculty of Life Sciences, Kumamoto University, Kumamoto-shi, Kumamoto, Japan, **2** Department of Research on Blood and Biological Products, National Institute of Infectious Diseases, Musashi-Murayama-shi, Tokyo, Japan, **3** Department of Internal Medicine, Goethe-University Hospital, Frankfurt, Germany, **4** Center for Microarray Analysis, Tokyo Metropolitan Institute of Medical Science, Kamikitazawa, Tokyo, Japan, **5** Department of Microbiology and Cell Biology, Tokyo Metropolitan Institute of Medical Science, Kamikitazawa, Tokyo, Japan, **6** Transboundary Animal Diseases Center, Joint Faculty of Veterinary Medicine, Kagoshima University, Kagoshima, Japan, **7** Laboratory of Animal Hygiene, Joint Faculty of Veterinary Medicine, Kagoshima University, Kagoshima, Japan

Abstract

Hepatitis C virus (HCV) infection leads to the development of hepatic diseases, as well as extrahepatic disorders such as B-cell non-Hodgkin's lymphoma (B-NHL). To reveal the molecular signalling pathways responsible for HCV-associated B-NHL development, we utilised transgenic (Tg) mice that express the full-length HCV genome specifically in B cells and develop non-Hodgkin type B-cell lymphomas (BCLs). The gene expression profiles in B cells from BCL-developing HCV-Tg mice, from BCL-non-developing HCV-Tg mice, and from BCL-non-developing HCV-negative mice were analysed by genome-wide microarray. In BCLs from HCV-Tg mice, the expression of various genes was modified, and for some genes, expression was influenced by the gender of the animals. Markedly modified genes such as Fos, C3, LTβR, A20, NF-κB and miR-26b in BCLs were further characterised using specific assays. We propose that activation of both canonical and alternative NF-κB signalling pathways and down-regulation of miR-26b contribute to the development of HCV-associated B-NHL.

Citation: Kasama Y, Mizukami T, Kusunoki H, Peveling-Oberhag J, Nishito Y, et al. (2014) B-Cell-Intrinsic Hepatitis C Virus Expression Leads to B-Cell-Lymphomagenesis and Induction of NF-κB Signalling. PLoS ONE 9(3): e91373. doi:10.1371/journal.pone.0091373

Editor: Ranjit Ray, Saint Louis University, United States of America

Received December 16, 2013; **Accepted** February 10, 2014; **Published** March 20, 2014

Funding: This work was supported by grants from the Ministry of Education, Culture, Sports, Science and Technology of Japan (23590547) and the Ministry of Health, Labour and Welfare of Japan (H21-011). The funders had no role in study design, data collection and analysis, decision to publish, or preparation of the manuscript.

Competing Interests: The authors have declared that no competing interests exist.

* E-mail: kkohara@vet.kagoshima-u.ac.jp

Introduction

Approximately 200 million people are currently infected with the hepatitis C virus (HCV) worldwide [1]. HCV has been the major etiological agent of post-transfusion hepatitis and has frequently caused liver cirrhosis and hepatocellular carcinoma in chronic hepatitis C (CHC) patients [2,3]. Hepatocytes are considered to be the primary and major site of HCV replication; however, extrahepatic manifestations are commonly seen in CHC patients. For example, mixed cryoglobulinemia (MC), a systemic immune complex-mediated disorder characterised by B cell proliferation with the risk of evolving into overt B-cell non-Hodgkin's lymphoma (B-NHL), is frequently recognised in CHC patients [4–6]. We have previously demonstrated the presence of both HCV RNA and viral proteins in peripheral B cells of CHC patients [7], although the mode of HCV infection and possible HCV replication in peripheral B cells remains a matter of debate. Furthermore, in the last two decades, an array of epidemiological evidence has accumulated involving the association between HCV infection and the occurrence of several hematologic malignancies, most notably B-NHL [8], [9]. The most compelling argument for a causal relationship between HCV and the occurrence of B-NHL is made by interventional studies demonstrating that a sustained virologic response to antiviral treatments, including the interferon α-induced regression of HCV-associated lymphomas and viral relapse after the initial virologic response, led to lymphoma recurrence [10]. However, the mechanisms underlying the cause-and-effect relationship are mostly unknown.

One of the potential host factors involved in HCV-associated B-NHL development is activator protein 1 (AP-1), which is primarily composed of c-Jun, c-Fos, and JunB, while JunD or Fra-1, Fra-2 and FosB are involved less frequently [11]. AP-1 is involved in B cell lymphomagenesis, is repressed by B cell lymphoma-6 [12] and is inhibited by the overexpression of T cell leukaemia/lymphoma 1, which resulted in the enhancement of nuclear factor kappa B (NF-κB) [13].

NF-κB is a ubiquitously expressed transcription factor that regulates a wide array of cellular processes, including the immune response, cell growth and differentiation [14,15]. The activation of NF-κB is regulated by two distinct pathways termed the 'canonical' and the 'alternative' NF-κB signalling pathways. Representative stimulators of the canonical and alternative pathways are tumour necrosis factor αTNFα) and lymphotoxin α and β (LTα and LTβ), respectively [16]. Previous studies have demonstrated that NF-κB is activated via both the canonical [17,18] and alternative [19] pathways in chronic HCV infection

[17,18] and HCV-related B-NHL [20]. However, the key NF-κB-activating pathway involved in HCV-associated B-NHL remains unknown.

TNFα-induced protein 3 (TNFAIP3), also known as A20, was first identified as a TNF-induced cytoplasmic protein with zinc finger motifs [21]. A20 has since been described as playing a pivotal role in the negative regulation of inflammation by terminating the canonical NF-κB signalling pathway [22–24]. Recently, A20 has gained attention as a novel tumour suppressor. For example, A20 was reported to be frequently inactivated or even deleted from mantle-cell lymphoma [25,26] and diffuse large B-cell lymphoma (DLBCL) [27]. These findings raise the possibility that inactivation of A20 is, at least partially, responsible for lymphomagenesis [28–30]. Other investigators have subsequently confirmed these findings [27,31]. Moreover, A20 also regulates antiviral signalling [32] as well as programmed cell death [33–35].

microRNAs (miRNAs) play a role in controlling various biological functions, including cell differentiation, growth regulation and transcriptional regulation [36]. In general, the dysfunctional expression of miRNAs is considered to be a common hallmark of cancers, including lymphomas [37]. HCV has been shown to influence miRNA expression *in vivo* and *in vitro* and utilises the liver-specific microRNA miR-122 for its replication [38]. The expression of miRNAs is also known to involve NF-κB activation. For example, miR-125a and miR-125b, both of which are often duplicated and/or overexpressed in DLBCL, were shown to activate NF-κB by targeting the A20 [39] and NF-κB-mediated dysregulation of miRNAs observed in lymphoma[40]. Moreover, global miRNA expression profiling analysis revealed miR-26b down-regulation in HCV-related splenic marginal zone lymphomas (SMZL) [41]. The same miRNA was found to be downregulated in peripheral blood mononuclear cells (PBMCs) from HCV-positive MC and NHL subjects [42].

We recently established transgenic mice that express the full-length HCV genome specifically in B cells (HCV-Tg mice) and observed the incidence of non-Hodgkin type B-cell lymphoma (BCL), primarily DLBCL, within 600 days after birth in approximately 25% of the HCV-Tg mice [43]. This experimental model is a useful tool for analysing the mechanisms underlying the development of HCV-associated manifestations such as B-NHL. To reveal the molecular signalling pathways responsible for HCV-associated B-NHL development, we performed a comprehensive molecular analysis of BCLs in HCV-Tg mice using a genome-wide microarray. We also characterised miR-26b expression in BCLs from HCV-Tg mice. Our results suggest that the activation of both canonical and alternative NF-κB pathways is involved in HCV-associated B-NHL development.

Materials and Methods

Ethics Statement

This study was carried out in strict accordance with both the Guidelines for Animal Experimentation of the Japanese Association for Laboratory Animal Science and the Guide for the Care and Use of Laboratory Animals of the National Institutes of Health. All experiment protocols were approved by the institutional review boards of the regional ethics committees of Kumamoto University (A22-136) and Kagoshima University (H24-008).

Animal experiments

The full-length HCV genome (Rz) under the conditional Cre/*lox*P expression system [44] with mice expressing the Cre enzyme under the transcriptional control of the B lineage–restricted gene *CD19* [45] was established as RzCD19Cre mice [43]. Wild-type (WT), Rz, CD19Cre, RzCD19Cre mice (129/sv, BALB/c and C57BL/6J mixed background) were maintained in conventional animal housing under specific pathogen-free conditions. CD19Cre and RzCD19Cre mice were bred to be heterozygous for the *Cre* allele.

Isolation of B cells and their RNAs

Mouse B cells were isolated using MACS^R beads (Milteny Biotec, Bergisch Gladbach, Germany) and anti-CD19 antibody (Beckton Dickinson, Franklin Lake, NJ). For FACS analysis, B and T cell populations were characterised using FITC-conjugated anti-B220 antibody (Milteny Biotec) and phycoerythrin (PE)-conjugated anti-CD3 antibody (Milteny Biotec) (Figure S1A). B cell purity was routinely over 95%. Total RNA was extracted from the B cells using the acid guanidine thiocyanate phenol chloroform method [44,46]. The RNA integrity number was measured with an Agilent 2100 Bioanalyzer (Agilent Technologies, Santa Clara, CA), and samples with values over 8.0 were subjected to microarray analysis (Figure S1B).

Microarray analysis

For microarray analysis, total RNAs were extracted, and RNA integrity was assessed using a Bioanalyzer (Agilent Technologies). cRNA targets were synthesised and hybridised with Whole Mouse Genome Microarray (G4846A; Agilent Technologies), in accordance with the manufacturer's instructions. More than 2-fold changes in gene expression were considered to be significant. Array data were analysed using MetaCore^{TM} software (Thomson Reuters Co., New York, NY). The results of microarray analysis

Table 1. Mice subjected to microarray analysis.

Pairing	Mouse genotype	Mouse (No)	Age (d)	Sex	Remarks
1	RzCD19Cre	24–1	748	male	HCV(+)BCL*
		59–1	723	male	
		69–5	710	male	
	RzCD19Cre	248–1	860	male	HCV(+) B cell
		288–3	472	male	
		299–1	385	male	
2	RzCD19Cre	307–2	212	male	HCV(+) B cell
		307–3	212	male	
	Rz, 4EBP(+/−)+	307–1	220	male	HCV(−) B cell
		312–1	220	male	
3	RzCD19Cre	54–1	724	female	HCV(+)BCL
		62–2	723	female	
	RzCD19Cre	308–4	219	female	HCV(+) B cell
		308–6	219	female	
4	RzCD19Cre	308–4	219	female	HCV(+) B cell
		308–6	219	female	
	Rz	308–1	219	female	HCV(−) B cell
		308–3	219	female	

*BCL: B cell lymphoma; +4EBP(+/−): heterozygous knockout of 4E-BP1 gene [73].

doi:10.1371/journal.pone.0091373.t001

A Disease network

Pairing 1 (HCV+B vs HCV+BCL, male)

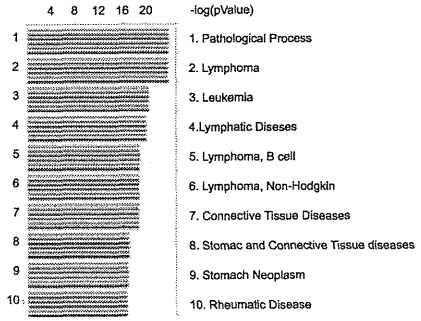

Pairing 2 (HCV+ vs HCV-, B cells, male)

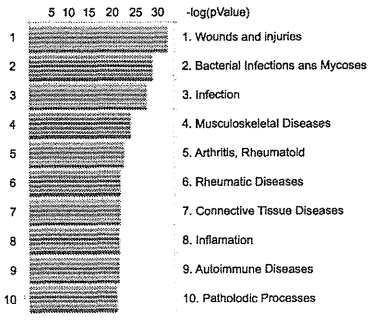

Pairing 3 (HCV+B vs HCV+BCL, female)

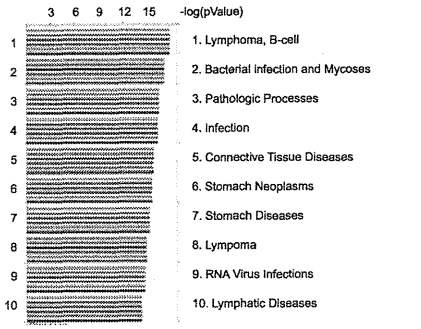

Pairing 4 (HCV+ vs HCV-, B cells, female)

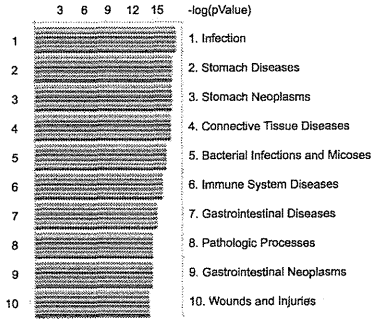

B Process network

Pairing 1 (HCV+B vs HCV+BCL, male)

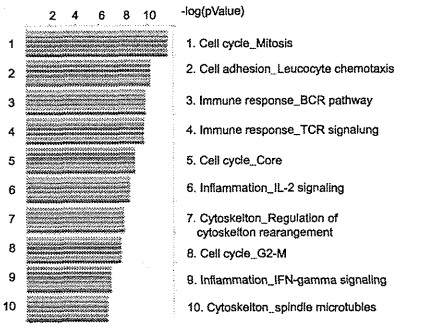

Pairing 2 (HCV+ vs HCV-, B cells, male)

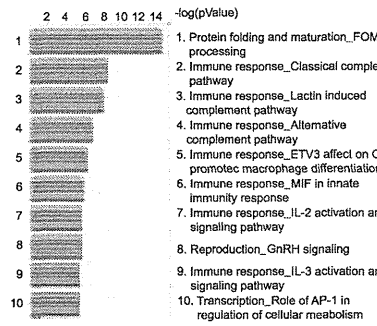

Pairing 3 (HCV+B vs HCV+BCL, female)

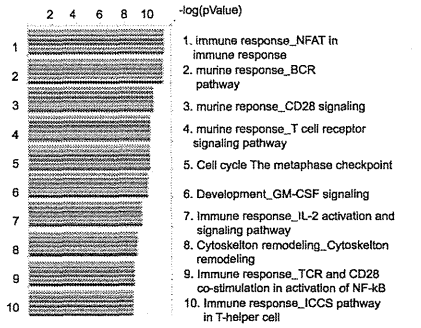

Pairing 4 (HCV+ vs HCV-, B cells, female)

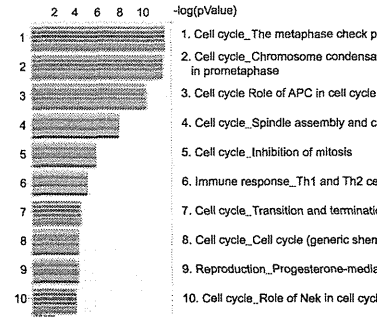

Figure 1. Data from array performed once with mixed RNA samples (Table 1) were analysed using MetaCore software. Signals were analysed in the disease network (**A**) and in the process network (**B**) the values for the microarray data [(Feature number; yellow), (Process Signal (635); blue), (Process signal (532); red), Test/Control (532/635); green], (Process Signal (635); orange), (Process signal (532); purple)] are indicated by coloured bars. Abbreviations: BCL = B cell lymphoma. Refer to Table 1 for construction of pairings.
doi:10.1371/journal.pone.0091373.g001

were registered in the Gene Expression Omnibus (GEO) database under the accession number GSE54722.

Quantitative RT-PCR

cDNA was synthesised from 0.5 or 1 μg of total RNA with a Superscript II kit (Life Technologies, Carlsbad, CA). TaqMan gene expression assays were custom-designed and manufactured by Life Technologies. RNA expression was quantified using the ABI 7500 real-time PCR system (Life Technologies) or the CFX96 system (BioRad, Hercules, CA).

Western blot analysis

Whole-cell proteins were extracted using RIPA buffer. Protein concentrations were determined using the BCA Protein assay Kit-Reducing Agent Compatible (Pierce Biotechnology, Rockford, IL). Samples (~10 μg) were loaded onto 10% SDS acrylamide gels, and gels were then transferred to PVDF membranes (Merck Millipore, Darmstadt, Germany). Membranes were blocked using 5% (w/v) non-fat milk for approximately 1 hour at room temperature and were then sequentially probed with primary and secondary antibodies at 4°C overnight and at room temperature for approximately 1 hour, respectively.

As primary antibodies, anti-A20 antibody (sc-166692; Santa Cruz Biotech, Dallas, TX), anti-A20 antibody (SAB3500036; Sigma-Aldrich, St. Louis, MO), anti-C3 antibody (D-19; Santa Cruz Biotech), anti-Fos (sc-52; Santa Cruz Biotech), anti-c-Jun(N) (sc-45; Santa Cruz Biotech) and anti-GAPDH-HRP (sc-20357; Santa Cruz Biotech) antibodies were used. Secondary antibodies used were horseradish peroxidase-coupled donkey anti-rabbit Ig (NA934; GE Healthcare, Buckinghamshire, UK) and horseradish peroxidase-coupled sheep anti-mouse Ig (NA931; GE Healthcare). Protein bands were detected and quantified using either Super-Signal West Dura or Femto Extended Duration Substrate (Pierce Biotechnology) with a LAS-3000 Image Analyzer (Fuji Film, Tokyo, Japan). Stripping and re-probing of the Western blots were performed using Re-blot plus mild antibody stripping solution (Merck Millipore).

Histological preparation

Liver, spleen, thymus and lymph nodes were harvested from HCV-Tg mice and fixed in 4% (wt/vol) paraformaldehyde in phosphate-buffered saline (pH 7.5) at 4°C for 24 hours. After fixation, samples were dehydrated in a graded ethanol series, cleared in xylene and embedded in paraffin, and 4-μm semi-thin sections were prepared using a carbon steel blade (Feather Safety Razor Co., Osaka, Japan) on a microtome (Yamato Kouki, Tokyo, Japan). Tissue sections were mounted on super-frosted glass slides coated with methyl-amino-silane (Matsunami Glass, Osaka, Japan). Histological images were acquired using an Olympus BX53 microscope (Olympus, Tokyo, Japan) equipped with 10×/0.30, 20×/0.50, 40×/0.75, and 100×/1.30 NA objective lenses. Images were captured using an Olympus DP73 (Olympus) under an Olympus FV1000 confocal microscope (Olympus).

Immunofluorescence

Anti-mouse NF-κB p65 antibody (Ab7970; Abcam, Cambridge, UK) and anti-mouse B220 (14-0452-81; eBioscience, San Diego, CA) were used as primary antibodies, and donkey anti-rat IgG-Alexa Fluor 488 [712-545-153; Jackson ImmunoResearch Laboratories Inc. (JIR), West Grove, PA], donkey anti-rabbit IgG-Alexa Fluor 488 (711-545-152; JIR), donkey anti-rat IgG-Cy3 (712-165-153; JIR) and donkey anti-rabbit IgG-Cy3 (711-165-152; JIR) were used as secondary antibodies. Staining was conducted as described previously [47]. Briefly, antigen retrieval was performed in a steam pressure cooker with prewarmed antigen retrieval buffer, citrate pH 6 (S203130; Dako, Glostrup, Denmark) at 95°C for 15 min. After blocking with 3% bovine serum albumin in phosphate-buffered saline, sections (4 μm) were incubated with anti-NF-κB, -Iκ-B, -B200 or -A20 antibodies at a 1:200 dilution each at 4°C overnight. Sections were incubated with secondary antibodies and anti-rat Alexa Fluor 488, -rabbit Alexa Fluor 488, -rat Alexa Fluor 546, and -rabbit Alexa Fluor 546 at room temperature for 2 hours. Nuclei were stained with Hoechst 333421 (H3570; Life Technologies).

Single assay stem-loop Q-RT-PCR/ miR-26b analysis

Formalin-fixed, paraffin-embedded (FFPE) splenic tissue from 24 animals (BCL HCV+, n = 8; BCL HCV-, n = 5; non-tumorous spleen HCV+/−, n = 11) was selected for miR-26b expression analysis. Total RNA was extracted using an RNeasy FFPE Kit (Qiagen, Hilden, Germany) in accordance with the manufacturer's protocol. Single assay stem-loop Q-RT-PCR (TaqMan MicroRNA assays, Life Technologies) was used to quantify miRNAs in accordance with the manufacturer's protocol. Total RNA input for each reaction was 50 ng. Expression was analysed for hsa-miR-26b and an endogenous control (snoRNA202). Each sample was analysed in triplicate, and delta C_t values were calculated using endogenous controls.

Statistics

For statistical analysis of NF-κB localisation, approximately 30–100 cells were randomly selected from each section area (two sections were used), and the cells double-positive for NF-κB and B220 were counted. All statistical analyses were performed using Prism software, version 5 (GraphPad, San Diego, CA). All experiments were independently performed three times, and a two-tailed Student *t*-test was applied to verify whether the results were significantly changed compared to the control ($P<0.05$).

Results

Characterisation of gene expression in B cells from HCV-Tg mice by microarray analysis

We previously established HCV-Tg mice that develop spontaneous BCL with a high penetrance (approximately 25%) [43]. To clarify the mechanisms of the HCV-associated B-NHL development using this mouse model, we performed a comprehensive gene expression analysis using a genome-wide microarray. B cells were isolated from BCL-developing HCV-Tg mice (Table 1, upper columns of pairing 1 and 3), from BCL-non-developing HCV-Tg mice (lower columns of pairing 1 and 3 and upper columns of pairing 2 and 4), and from BCL-non-developing HCV-negative mice (lower columns of pairing 2 and 4). RNA was purified from these B cells (Figure S1) and was characterised by microarray analysis (data not shown). In B cells isolated from BCL-non-developing HCV-Tg male mice, 455 and 863 genes were up-

A

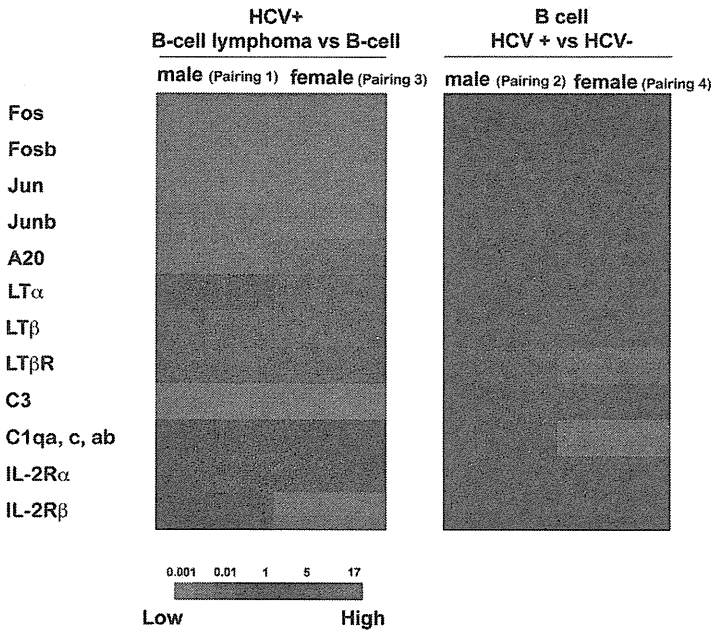
HCV+
B-cell lymphoma vs B-cell
B cell
HCV + vs HCV-
male (Pairing 1) female (Pairing 3)
male (Pairing 2) female (Pairing 4)
Fos
Fosb
Jun
Junb
A20
LTα
LTβ
LTβR
C3
C1qa, c, ab
IL-2Rα
IL-2Rβ
0.001 0.01 1 5 17
Low
High

B

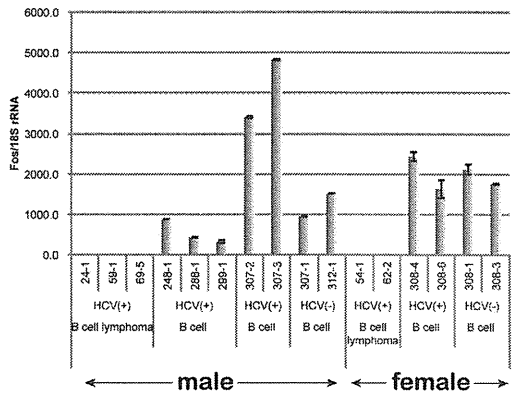
Fos/18S rRNA
6000.0
5000.0
4000.0
3000.0
2000.0
1000.0
0.0
24-1 59-1 69-5 248-1 288-1 289-1 307-2 307-3 307-1 312-1 54-1 62-2 308-4 308-6 308-1 308-3
HCV(+) B cell lymphoma
HCV(+) B cell
HCV(+) B cell
HCV(-) B cell
HCV(+) B cell lymphoma
HCV(+) B cell
HCV(-) B cell
male
female

C

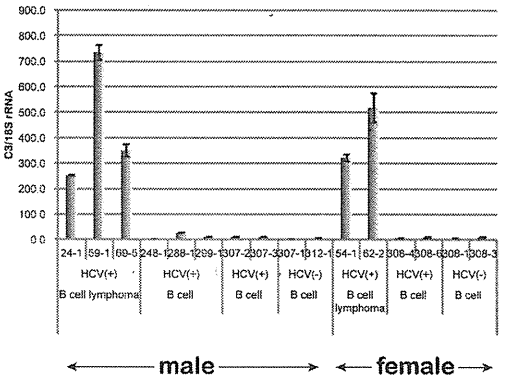
C3/18S rRNA
900.0
800.0
700.0
600.0
500.0
400.0
300.0
200.0
100.0
0.0
24-1 59-1 69-5 248-1 288-1 289-1 307-2 307-3 307-1 312-1 54-1 62-2 308-4 308-6 308-1 308-3
HCV(+) B cell lymphoma
HCV(+) B cell
HCV(+) B cell
HCV(-) B cell
HCV(+) B cell lymphoma
HCV(+) B cell
HCV(-) B cell
male
female

D

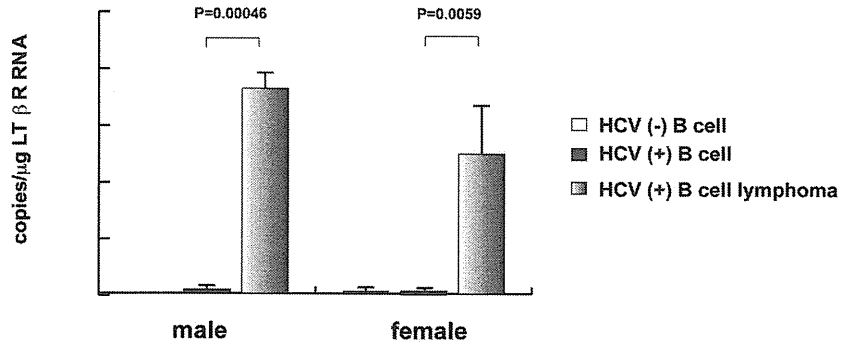
copies/μg LT β R RNA
P=0.00046
P=0.0059
male
female
HCV (-) B cell
HCV (+) B cell
HCV (+) B cell lymphoma

Figure 2. The expression of genes involved in oncogenic pathways associated with BCL. A: Highly modified gene signals in B cell lymphoma in RzCD19Cre mice BCL vs. B cells in RzCD19Cre male (Pair 1) or female (Pair 3) mice (left), and the genes modified by HCV expression in B cells in male (Pair 2) or female (Pair 4) (right). Red indicates the relative enhancement of the expression ratio of the processed signal (Test/Control, 532/635), and green indicates the relative reduction of expression. **B**: Quantification of Fos mRNA in HCV-, HCV+ B cells and HCV-Tg BCL in mice (numbers of individual mice were indicated) by quantitative RT-PCR. Fos mRNA was normalised against 18S rRNA, and the relative ratio was calculated. Vertical bars indicate S.D. **C**: Quantification of C3 mRNA in HCV-, HCV+ B cells and HCV-Tg BCL in mice. C3 mRNA was normalised against 18S rRNA, and relative ratio was calculated. Vertical bars indicate S.D. **D**: Quantification of LT βR mRNA in HCV-, HCV+ B cells and HCV-Tg BCL in mice by quantitative RT-PCR. RNA copies per total RNA (μg) were indicated and vertical bars indicate S.D.
doi:10.1371/journal.pone.0091373.g002

and down-regulated, respectively, compared with the HCV-negative counterparts (Table 1, pairing 2); whereas 133 and 331 genes were up- and down-regulated, respectively, in BCL-non-developing HCV-Tg female mice (Table 1, pairing 4). Furthermore, 1,682 and 2,383 genes were up- and down-regulated, respectively, in BCL-developing HCV-Tg male mice compared to their BCL-non-developing counterparts (Table 1, pairing 1); whereas 2,089 and 2,565 genes were up- and down-regulated, respectively, in BCL-developing HCV-Tg female mice (Table 1, pairing 3).

Metacore analysis of microarray results

In order to characterize the cellular processes affected by the gene expression changes, we carried out a pathway analysis of microarray data of pairings 1–4 (Table 1) using MetaCore™ software. This data mining revealed that lymphoma, leukaemia, B cell lymphoma, and lymphatic disease pathways were appreciably modified in pairings 1 and 3 with high frequency (Figure 1a). In pairings 2 and 4, the modifications involving wound healing and infection pathways were highlighted, respectively. In the process network, the cell cycle and immune response (B cell receptor, T cell receptor, and IL-2) pathways were greatly modified in pairings 1 and 3 (Figure 1b). The immune response (complement, macrophage, IL-2, and IL-3 in group 2; Th1 and Th2 in pairing), protein folding (in pairing 2), and cell cycle (in pairing 4) pathways were also modified.

Dysregulated genes in HCV-associated B-cell lymphoma

In addition to the pathways analysis, we also carefully examined the expression of genes involved in oncogenic pathways associated with BCL. Expression of Fos, Fosb, Jun and Junb was markedly down-regulated in BCL obtained from HCV-Tg mice (Figure 2a). Similarly, the expression of A20 and LTβ was greatly down-regulated in BCL (Figure 2a). In contrast, the expression of the LTβ receptor (LTβR), the IL-2 receptor α(IL-2Rα, IL-2Rβ and complement C3 was up-regulated in the examined BCLs (Figure 2a). While alterations in the gene expression of LTα and IL-2Rβ differed between males and females, the overall mRNA expression profile in the BCL analysed from HCV-Tg mice essentially showed no differences between male and female mice. In addition, clinically, there was no clear gender priority in HCV-NHL [48–50]. These results suggest that the molecular signalling pathways leading to HCV-associated B-NHL development are common to males and females.

In non-tumorous B cells from BCL-non-developing HCV-Tg male mice, the expression of LTβR and C3 was up-regulated when compared with HCV-negative counterparts (Figure 2a). In contrast, in female counterparts, the expression of LTβR and complements C1qa, c, and ab was down-regulated (Figure 2a, Pair. 4). These results suggest that the impact of HCV infection in B cells may be different between males and females.

Expression of Fos, C3, and LTβR genes in HCV-associated BCL

In order to validate the microarray results, levels of Fos and C3 mRNAs were quantified by real-time PCR. Striking down-regulation of Fos gene expression was observed in BCLs from HCV-Tg mice (Figure 2b). In contrast, C3 mRNA expression was markedly up-regulated in BCLs from HCV-Tg mice (Figure 2c). These results were consistent with the microarray data (Figure 2a, GEO accession number GSE54722). Similarly, the mRNA expression of the LTβR gene was significantly increased in HCV-associated BCLs (Figure 2d), confirming the microarray analysis results (Figure 2a). Importantly, these changes occurred in both male and female mice.

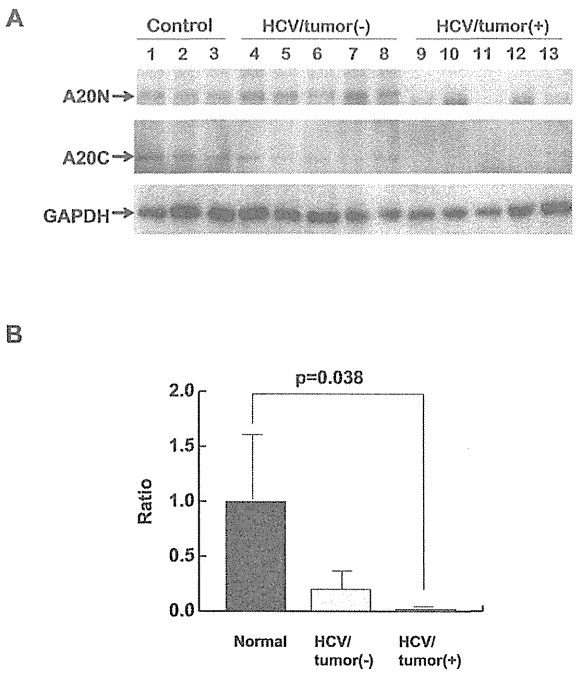

Figure 3. The expression of A20 in HCV-associated BCL. A: Expression levels of A20 in the spleen from RzCD19Cre mice with or without BCL. Whole-tissue extracts prepared from the spleen in CD19Cre mice (control, n = 3; lanes 1–3 217–2, 2 224–2, 224–3), RzCD19Cre mice without BCL (HCV/Tumour(-), n = 5; lanes 4–8 217–3, 224–4, 232–3, 254–4, 240–2) and RzCD19Cre mice with BCL (HCV/Tumour(+), n = 5; lanes 9–13 24–1, 56–5, 69–5, 59–1, 43–4) were subjected to SDS-PAGE and were analysed by immunoblotting using anti-N terminal (A20N), anti-C terminal A20 (A20C), and anti-GAPDH antibodies. GAPDH was used as protein loading control. **B**: Quantitation of A20 (N and C), the average is indicated and statistical analysis was performed. Vertical bars indicate S.D.
doi:10.1371/journal.pone.0091373.g003

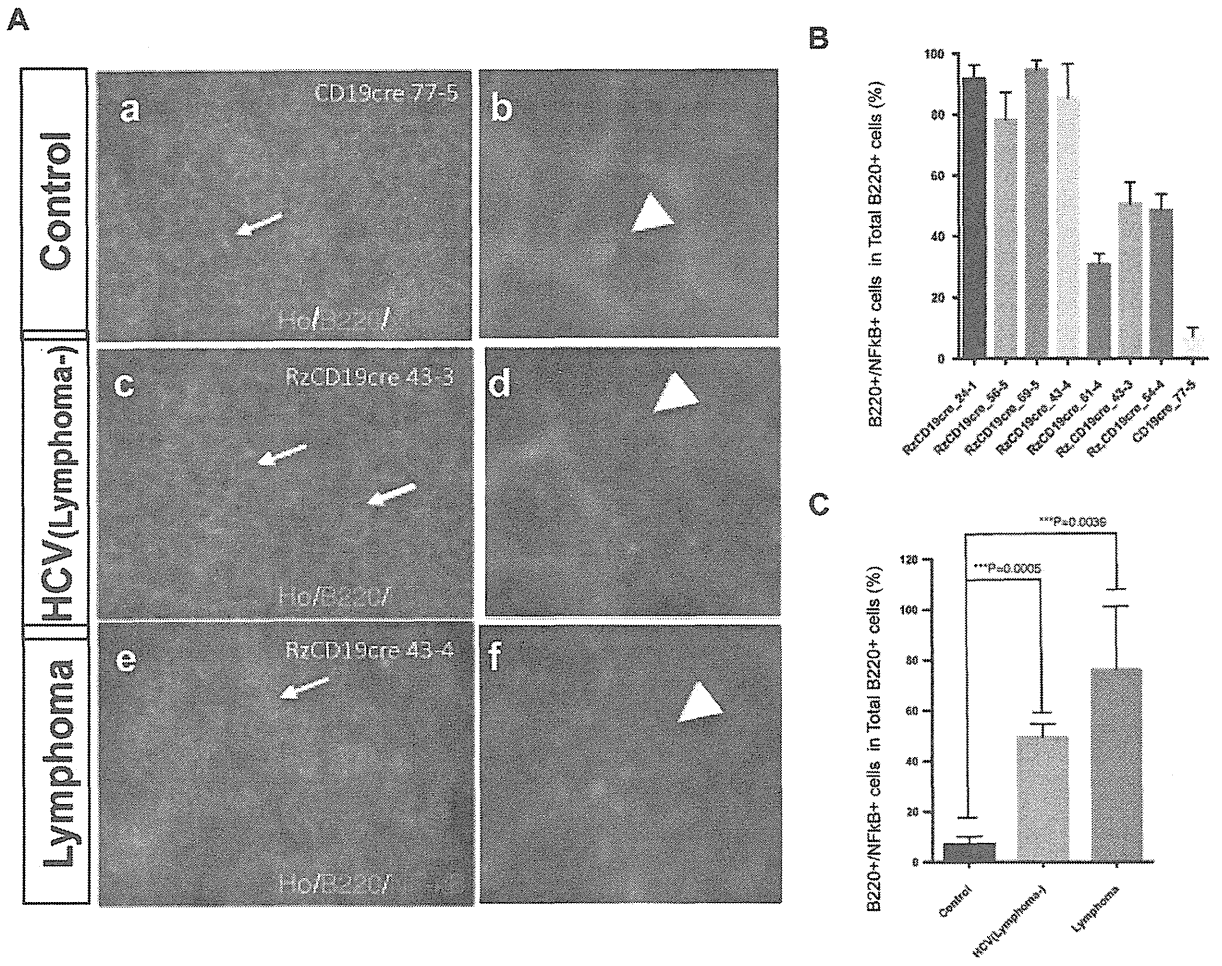

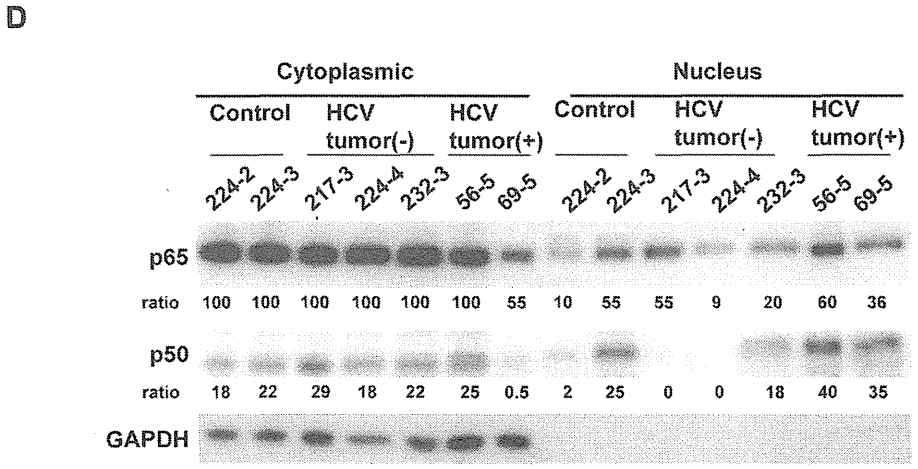

Figure 4. Double immunofluorescence localisation of B220 (Green) and NF-κB p65 (Red) in HCV-Tg mice and the fractionation analysis of mouse tissues. A: Co-localisation of NF-κB p65 immunoreactivity with B220 is indicated by arrows. (a–b) Cells double-positive for B220 and NF-κB in the control mouse (CD19cre). (c–d) Cells double-positive for B220 and NF-κB in the asymptomatic HCV-Tg mouse (RzCD19cre). (e–f) Cells double-positive for B220 and NF-κB in the lymphomatous HCV-Tg mouse (RzCD19cre). **B**: Quantitative analysis of the ratio of double-positive

cells among B220-positive cells in each HCV-Tg mouse. Bar graph indicates the percentage of cells with NF-κB p65 nuclear translocation in B220-positive cells. **C**: Bar graph shows the ratio of double-positive cells within the B220-positive cells in normal, asymptomatic and lymphomatous HCV-Tg mice. Ho: Hoechst33342 Data are presented as means ± S.E., * $P<0.05$, ** $P<0.01$, *** $P<0.001$. **D**: Western blot analysis: tissues from the spleen of controls (224–2, 3) or HCV-Tg mice without BCL (217–3, 224–4, 232–3) or with BCL (56–5, 69–5) were fractionated into nuclear and cytoplasmic fractions. NF-κB p50 and p65 were detected by antibodies. Relative ratios of quantitation by imager are indicated. GAPDH was detected as a loading control of the cytoplasmic fraction.
doi:10.1371/journal.pone.0091373.g004

Expression of A20 in HCV-associated BCL

In order to further validate the microarray results, we assessed A20 protein levels in BCLs isolated from HCV-Tg mice by Western blotting (Figure 3a). Two distinct anti-A20 antibodies recognising the N- (A20N) and C-terminal regions were used for the detection of A20. Regardless of the anti-A20 antibodies used, expression levels of A20 in BCL from HCV-Tg mice (Figure 3a, lanes 9 to 13) were markedly decreased when compared to splenocytes obtained from either BCL-non-developing HCV-negative mice (lanes 1 to 3) or from BCL-non-developing HCV-Tg mice (lanes 4 to 8). Quantitative analysis showed a significant decrease in A20 in BCLs obtained from HCV-Tg mice (Figure 3b). These results strongly suggest that the reduced expression of A20 is correlated with HCV-associated N-BHL development.

Nuclear localisation of NF-kB p65 in HCV-associated BCL

We next analysed the activation status of NF-κB by investigating the nuclear localisation of NF-κB p65 in cells positive for a B-cell marker molecule, B220, in BCLs isolated from HCV-Tg mice (Figure 4a). Quantitative analysis revealed that the ratio of cells double-positive for B220 and NF-κB p65 in the nuclei of the examined BCLs was significantly higher than the ratio in splenic tissue obtained from either BCL-non-developing HCV-negative mice or from BCL-non-developing HCV-Tg mice (Figures 4b and c). The fractionation assay showed that more NF-κB p50 and p65 were present in BCLs from HCV-Tg mice (Figure 4d). These results indicate the activation of NF-κB in HCV-associated BCL.

Expression of miR-26b in HCV-associated BCL

Recent studies have demonstrated that miR-26b is down-regulated in hepatocellular carcinoma [51], nasopharyngeal carcinoma [52], primary squamous cell lung carcinoma [53] and squamous cell carcinoma of the tongue [54]. In addition, miR-26b was down-regulated in HCV-positive SMZL when compared with HCV-negative counterparts [41] and in the PBMC of HCV-positive MC and NHL patients [42]. Therefore, we compared the expression levels of miR-26b in BCL from HCV-Tg mice with BCL from HCV-negative mice (i.e., spontaneously developed BCL) or in splenic tissue from BCL non-developing HCV-positive and -negative mice (Figure. 5). Interestingly, miR-26b expression was significantly down-regulated in BCLs from HCV-Tg mice. These results indicate that miR-26b is also down-regulated in HCV-associated BCL.

Discussion

In the present study, we identified differentially expressed genes in BCLs examined from HCV-Tg mice using a genome-wide microarray (Figures 1 and 2a, Table 1, and Figure S2). The microarray results for representative genes were validated at the RNA (Figures 2 and 5) and protein (Figures 3 and 4) levels. These findings helped dissect the molecular mechanisms underlying HCV-associated B-NHL development.

In the BCLs from HCV-Tg mice, the marked down-regulation of the Fos gene as well as other AP-1 protein genes (Fosb, Jun and Junb) was observed. Although AP-1 DNA binding activity was observed in Hodgkin-/multinuclear Reed-Stemberg cells and tissues from classical Hodgkin's disease, non-Hodgkin cell lines lacked the DNA binding activity of AP-1 [55]. Junb was weakly expressed in non-Hodgkin lymphomas of B-lymphoid origin; however, strong expression has been previously found in lymphomas that originated from the T-lymphoid lineage, and Junb selectively blocked B-lymphoid but not T-lymphoid cell proliferation ex vivo [56]. The BCL that developed in HCV-Tg mice was the non-Hodgkin type [43]; therefore, the decrease in AP-1 protein levels (Fos, Fosb, Jun, and Junb) may be crucial for lymphoma development.

In our previous study, soluble IL-2Rα levels were increased in BCL-developing HCV-Tg mice [43] Therefore, the up-regulation of IL-2Rα(Figure 2a) is potentially linked to the increase of soluble IL-2Rα, although further investigation is needed to clarify the details of this mechanism.

Expression of complement component C3 was significantly increased in BCLs isolated from HCV-Tg mice (Figure 2c). The presence of polymorphisms in complement system genes in non-Hodgkin lymphoma [57] suggests the involvement of complement in lymphoma development. The elevated C3 expression may be induced by TNF-α [58]. In addition, C3a, which is a cleavage product of C3, may contribute to the binding of NF-κB and AP-1 as shown previously [59].

The expression of LTβR, which is one of the key molecules in the alternative NF-κB signalling pathway [16], was significantly increased in BCLs from HCV-Tg mice (Figure 2d). HCV core proteins were reported to interact with the cytoplasmic domain of LTβR [60,61] and to enhance the alternative NF-κB signalling pathway [62]. The induction of LTβR by the HCV non-structural protein NS5B, and HCV RNA-dependent RNA polymerase, was also observed [63]. These findings suggest that the regulatory pathways involved in HCV infection also play a role in HCV-associated B-NHL development.

We observed several differences in the gene expression between male and female mice. Male HCV-negative mice showed up-regulation of LTβR and C3; however, female HCV-positive mice featured the downregulation of LTα and up-regulation of IL-2Rβ. Female HCV-Tg mice showed decreased overall survival in a previous study [43] and the above-mentioned gene dysregulations may contribute to this finding. However, the incidence of B-NHL between male and female mice did not show marked differences in the transgenic model [43]. Some clinical studies found gender-specific differences in the incidence of HCV-associated B-NHL and different effects of HCV on gene expression, which may also be dependent on gender [64]. However, meta-analyses did not provide consistent evidence for any gender preferences in HCV-NHL [48–50].

The down-regulation of A20, which is a ubiquitin-editing enzyme and tumour suppressor in various lymphomas [26], was observed in BCLs from HCV-Tg mice (Figures 3a and 3b). A20 has been reported to interact with the TNF receptor associated factor 2 (TRAF2), TRAF6, and the NF-κB essential modulator (NEMO). A20 inhibits NF-κB activation-induced by TNFα or by the overexpression of other proteins such as TRAF2 and receptor-interacting protein serine/threonine kinase 1 (RIPK1) proteins

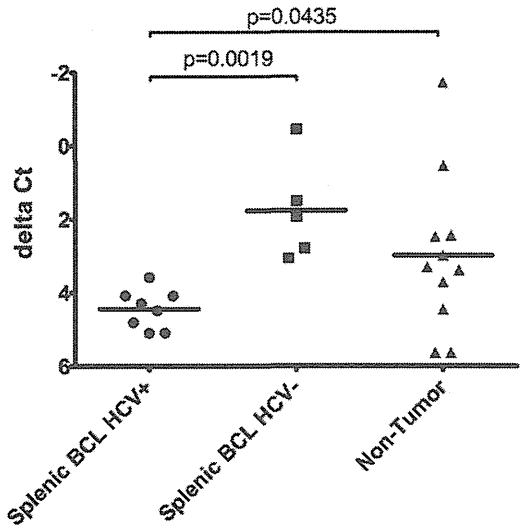

Figure 5. Quantification of miR-26b in BCL from HCV-positive and HCV-negative and non-tumour Tg mice. Formalin-fixed, paraffin-embedded (FFPE) splenic tissue from 24 animals (BCL HCV+, n = 8; BCL HCV-, n = 5; non-tumorous spleen HCV+/−, n = 11) was analysed for miR-26b expression by single assay stem-loop Q-RT-PCT by triplicate experiments. Data are shown as scatter dot-plots, and horizontal bar depicts the mean; y-axis: delta Ct (inverted scale) calculated in relation to endogenous control (snoRNA202). HCV-positive lymphoma tissue: filled circles; HCV-negative lymphoma tissue: filled squares; non-tumorous splenic tissue: filled triangles. P-values are shown in the graph.
doi:10.1371/journal.pone.0091373.g005

[65]. RIPK3 contributes to TNFR1-mediated RIPK1-dependent apoptosis and necroptosis [66]. RIPK2 (also known as RIP2) is also involved in B cell lymphoma cell survival and mediates the activation of NF-κB and MAPK pathways, associated with the TNF receptor family [67]. Therefore, suppression of A20 activates NF-κB by increasing nuclear translocation in tumour tissues.

Expression of miR-26b in BCLs obtained from HCV-Tg mice was significantly down-regulated (Figure 5). miR-26b is also down-regulated in numerous cancers, e.g., HCC [51], nasopharyngeal carcinomas [52], primary squamous cell lung carcinomas [53]and squamous cell carcinoma tongue [54]. In addition, c-Myc, which is up-regulated in various cancer types, has been shown to contribute to the reduction of miR-26a/b expression [68]. Notably, expression of miR-26b was significantly down-regulated in SMZL arising in HCV-positive patients [41]. Although the mechanisms of miR-26b-mediated tumourigenicity regulation are not fully understood, previous reports [69] and the present study have suggested a possible regulatory role of miR-26b in HCV-related lymphoma. Several candidates are reported to be targets of miR-26b. miR-26a and miR-26b are regulators of EZH2, which is the PRC2 polycomb repressive complex, is overexpressed in multiple cancers and is a target of the MYC oncogene [70]. In addition, lymphoid enhancer factor (LEF)-1 [42] and Nek6 [41] are targets of miR-26b. LEF-1 is a nuclear transcription factor that forms a complex with β-catenine and T-cell factor and induces transcription of cyclin D1 and c-myc. Nek6 is a kinase involved in the initiation of mitosis and is overexpressed in various tumours. The phosphatase and tensin homolog gene (PTEN) is also the putative target gene of miR-26b in adipogenic regulation [71] and cell growth [72].

This report is the first to demonstrate the possible involvement of networks of NF-κB, AP-1, complements and miR-26b in HCV-associated B-NHL (Figure S2). A future study focusing on the dysregulation of these networks and their modification by HCV may provide valuable information on improving therapy for HCV-associated B-NHL.

Supporting Information

Figure S1 **A**: B cells were isolated from mice using MACS beads and anti-CD19 antibody. The population of B cells was confirmed by staining with anti-B220 antibody. **B**: RNA integrity number (RIN) was measured using an Agilent 2100 Bioanalyzer (Agilent) for the estimation of purity.
(PDF)

Figure S2 Possible pathways involved in BCL development. Both canonical and alternative NF-κB pathways may play a role. Bold arrows indicate up-regulation or down-regulation. NIK; NF-κB-inducing kinase.
(PDF)

Acknowledgments

We would like to thank Drs. Kitabatake, Sato and Saito for their assistance with B cell separation and characterisation, and Professor Sakaguchi for his valuable encouragement.

Author Contributions

Conceived and designed the experiments: KT-K T. Mizuochi. Performed the experiments: YK T. Mizukami HK JP-O KT-K. Analyzed the data: YN JP-O T. Mizuochi KT-K. Contributed reagents/materials/analysis tools: MK. Wrote the paper: MO JP-O T. Mizuochi KT-K.

References

1. Shepard CW, Finelli L, Alter MJ (2005) Global epidemiology of hepatitis C virus infection. Lancet Infect Dis 5: 558–567.
2. Libra M, Gasparotto D, Gloghini A, Navolanic PM, De Re V, et al. (2005) Hepatitis C virus (HCV) I hepatitis C virus (HCV) infection and lymphoproliferative disorders. Front Biosci 10: 2460–2471.
3. Saito I, Miyamura T, Ohbayashi A, Harada H, Katayama T, et al. (1990) Hepatitis C virus infection is associated with the development of hepatocellular carcinoma. Proc Natl Acad Sci U S A 87: 6547–6549.
4. Silvestri F, Pipan C, Barillari G, Zaja F, Fanin R, et al. (1996) Prevalence of hepatitis C virus infection in patients with lymphoproliferative disorders. Blood 87: 4296–4301.
5. Ascoli V, Lo Coco F, Artini M, Levrero M, Martelli M, et al. (1998) Extranodal lymphomas associated with hepatitis C virus infection. Am J Clin Pathol 109: 600–609.
6. Mele A, Pulsoni A, Bianco E, Musto P, Szklo A, et al. (2003) Hepatitis C virus and B-cell non-Hodgkin lymphomas: an Italian multicenter case-control study. Blood 102: 996–999.
7. Ito M, Kusunoki H, Mizuochi T (2011) Peripheral B cells as reservoirs for persistent HCV infection. Front Microbiol 2: 177.
8. Dammacco F, Sansonno D, Piccoli C, Racanelli V, D'Amore FP, et al. (2000) The lymphoid system in hepatitis C virus infection: autoimmunity, mixed cryoglobulinemia, and Overt B-cell malignancy. Semin Liver Dis 20: 143–157.
9. Peveling-Oberhag J, Arcaini L, Hansmann ML, Zeuzem S (2013) Hepatitis C-associated B-cell non-Hodgkin lymphomas. Epidemiology, molecular signature and clinical management. J Hepatol 59: 169–177.
10. Hermine O, Lefrere F, Bronowicki JP, Mariette X, Jondeau K, et al. (2002) Regression of splenic lymphoma with villous lymphocytes after treatment of hepatitis C virus infection. N Engl J Med 347: 89–94.
11. Hess J, Angel P, Schorpp-Kistner M (2004) AP-1 subunits: quarrel and harmony among siblings. J Cell Sci 117: 5965–5973.
12. Vasanwala FH, Kusam S, Toney LM, Dent AL (2002) Repression of AP-1 function: a mechanism for the regulation of Blimp-1 expression and B lymphocyte differentiation by the B cell lymphoma-6 protooncogene. J Immunol 169: 1922–1929.

13. Pekarsky Y, Palamarchuk A, Maximov V, Efanov A, Nazaryan N, et al. (2008) Tcl1 functions as a transcriptional regulator and is directly involved in the pathogenesis of CLL. Proc Natl Acad Sci U S A 105: 19643–19648.
14. Ghosh S, Karin M (2002) Missing pieces in the NF-kappaB puzzle. Cell 109 Suppl: S81–96.
15. Sen R, Baltimore D (1986) Inducibility of kappa immunoglobulin enhancer-binding protein Nf-kappa B by a posttranslational mechanism. Cell 47: 921–928.
16. Bakkar N, Guttridge DC (2010) NF-kappaB signaling: a tale of two pathways in skeletal myogenesis. Physiol Rev 90: 495–511.
17. Sun B, Karin M (2008) NF-kappaB signaling, liver disease and hepatoprotective agents. Oncogene 27: 6228–6244.
18. Arsura M, Cavin LG (2005) Nuclear factor-kappaB and liver carcinogenesis. Cancer Lett 229: 157–169.
19. Haybaeck J, Zeller N, Wolf MJ, Weber A, Wagner U, et al. (2009) A lymphotoxin-driven pathway to hepatocellular carcinoma. Cancer Cell 16: 295–308.
20. De Re V, Caggiari L, Garziera M, De Zorzi M, Repetto O (2012) Molecular signature in HCV-positive lymphomas. Clin Dev Immunol 2012: 623465.
21. Opipari AW, Jr., Boguski MS, Dixit VM (1990) The A20 cDNA induced by tumor necrosis factor alpha encodes a novel type of zinc finger protein. J Biol Chem 265: 14705–14708.
22. Song HY, Rothe M, Goeddel DV (1996) The tumor necrosis factor-inducible zinc finger protein A20 interacts with TRAF1/TRAF2 and inhibits NF-kappaB activation. Proc Natl Acad Sci U S A 93: 6721–6725.
23. Lee EG, Boone DL, Chai S, Libby SL, Chien M, et al. (2000) Failure to regulate TNF-induced NF-kappaB and cell death responses in A20-deficient mice. Science 289: 2350–2354.
24. Heyninck K, Beyaert R (2005) A20 inhibits NF-kappaB activation by dual ubiquitin-editing functions. Trends Biochem Sci 30: 1–4.
25. Malynn BA, Ma A (2009) A20 takes on tumors: tumor suppression by an ubiquitin-editing enzyme. J Exp Med 206: 977–980.
26. Hymowitz SG, Wertz IE (2010) A20: from ubiquitin editing to tumour suppression. Nat Rev Cancer 10: 332–341.
27. Kato M, Sanada M, Kato I, Sato Y, Takita J, et al. (2009) Frequent inactivation of A20 in B-cell lymphomas. Nature 459: 712–716.
28. Honma K, Tsuzuki S, Nakagawa M, Karnan S, Aizawa Y, et al. (2008) TNFAIP3 is the target gene of chromosome band 6q23.3-q24.1 loss in ocular adnexal marginal zone B cell lymphoma. Genes Chromosomes Cancer 47: 1–7.
29. Honma K, Tsuzuki S, Nakagawa M, Tagawa H, Nakamura S, et al. (2009) TNFAIP3/A20 functions as a novel tumor suppressor gene in several subtypes of non-Hodgkin lymphomas. Blood 114: 2467–2475.
30. Schmitz R, Hansmann ML, Bohle V, Martin-Subero JI, Hartmann S, et al. (2009) TNFAIP3 (A20) is a tumor suppressor gene in Hodgkin lymphoma and primary mediastinal B cell lymphoma. J Exp Med 206: 981–989.
31. Compagno M, Lim WK, Grunn A, Nandula SV, Brahmachary M, et al. (2009) Mutations of multiple genes cause deregulation of NF-kappaB in diffuse large B-cell lymphoma. Nature 459: 717–721.
32. Parvatiyar K, Barber GN, Harhaj EW (2010) TAX1BP1 and A20 inhibit antiviral signaling by targeting TBK1-IKKi kinases. J Biol Chem 285: 14999–15009.
33. Parvatiyar K, Harhaj EW (2011) Regulation of inflammatory and antiviral signaling by A20. Microbes Infect 13: 209–215.
34. Tavares RM, Turer EE, Liu CL, Advincula R, Scapini P, et al. (2010) The ubiquitin modifying enzyme A20 restricts B cell survival and prevents autoimmunity. Immunity 33: 181–191.
35. Verstrepen L, Verhelst K, van Loo G, Carpentier I, Ley SC, et al. (2010) Expression, biological activities and mechanisms of action of A20 (TNFAIP3). Biochem Pharmacol 80: 2009–2020.
36. He L, Hannon GJ (2004) MicroRNAs: small RNAs with a big role in gene regulation. Nat Rev Genet 5: 522–531.
37. Lawrie CH (2007) MicroRNA expression in lymphoma. Expert Opin Biol Ther 7: 1363–1374.
38. Jopling CL, Yi M, Lancaster AM, Lemon SM, Sarnow P (2005) Modulation of hepatitis C virus RNA abundance by a liver-specific MicroRNA. Science 309: 1577–1581.
39. Kim SW, Ramasamy K, Bouamar H, Lin AP, Jiang D, et al. (2012) MicroRNAs miR-125a and miR-125b constitutively activate the NF-kappaB pathway by targeting the tumor necrosis factor alpha-induced protein 3 (TNFAIP3, A20). Proc Natl Acad Sci U S A 109: 7865–7870.
40. Hother C, Rasmussen PK, Joshi T, Reker D, Ralfkiaer U, et al. (2013) MicroRNA Profiling in Ocular Adnexal Lymphoma: A Role for MYC and NFKB1 Mediated Dysregulation of MicroRNA Expression in Aggressive Disease. Invest Ophthalmol Vis Sci 54: 5169–5175.
41. Peveling-Oberhag J, Crisman G, Schmidt A, Doring C, Lucioni M, et al. (2012) Dysregulation of global microRNA expression in splenic marginal zone lymphoma and influence of chronic hepatitis C virus infection. Leukemia 26: 1654–1662.
42. Fognani E, Giannini C, Piluso A, Gragnani L, Monti M, et al. (2013) Role of microRNA profile modifications in hepatitis C virus-related mixed cryoglobulinemia. PLoS One 8: e62965.
43. Kasama Y, Sekiguchi S, Saito M, Tanaka K, Satoh M, et al. (2010) Persistent expression of the full genome of hepatitis C virus in B cells induces spontaneous development of B-cell lymphomas in vivo. Blood 116: 4926–4933.
44. Tsukiyama-Kohara K, Tone S, Maruyama I, Inoue K, Katsume A, et al. (2004) Activation of the CKI-CDK-Rb-E2F pathway in full genome hepatitis C virus-expressing cells. J Biol Chem 279: 14531–14541.
45. Rickert RC, Roes J, Rajewsky K (1997) B lymphocyte-specific, Cre-mediated mutagenesis in mice. Nucleic Acids Res 25: 1317–1318.
46. Nishimura T, Kohara M, Izumi K, Kasama Y, Hirata Y, et al. (2009) Hepatitis C virus impairs p53 via persistent overexpression of 3beta-hydroxysterol Delta24-reductase. J Biol Chem 284: 36442–36452.
47. Yamazaki J, Mizukami T, Takizawa K, Kuramitsu M, Momose H, et al. (2009) Identification of cancer stem cells in a Tax-transgenic (Tax-Tg) mouse model of adult T-cell leukemia/lymphoma. Blood 114: 2709–2720.
48. Gisbert JP, Garcia-Buey L, Pajares JM, Moreno-Otero R (2003) Prevalence of hepatitis C virus infection in B-cell non-Hodgkin's lymphoma: systematic review and meta-analysis. Gastroenterology 125: 1723–1732.
49. Matsuo K, Kusano A, Sugumar A, Nakamura S, Tajima K, et al. (2004) Effect of hepatitis C virus infection on the risk of non-Hodgkin's lymphoma: a meta-analysis of epidemiological studies. Cancer Sci 95: 745–752.
50. de Sanjose S, Benavente Y, Vajdic CM, Engels EA, Morton LM, et al. (2008) Hepatitis C and non-Hodgkin lymphoma among 4784 cases and 6269 controls from the International Lymphoma Epidemiology Consortium. Clin Gastroenterol Hepatol 6: 451–458.
51. Ji J, Shi J, Budhu A, Yu Z, Forgues M, et al. (2009) MicroRNA expression, survival, and response to interferon in liver cancer. N Engl J Med 361: 1437–1447.
52. Ji Y, He Y, Liu L, Zhong X (2010) MiRNA-26b regulates the expression of cyclooxygenase-2 in desferrioxamine-treated CNE cells. FEBS Lett 584: 961–967.
53. Gao W, Shen H, Liu L, Xu J, Xu J, et al. (2011) MiR-21 overexpression in human primary squamous cell lung carcinoma is associated with poor patient prognosis. J Cancer Res Clin Oncol 137: 557–566.
54. Wong TS, Liu XB, Wong BY, Ng RW, Yuen AP, et al. (2008) Mature miR-184 as Potential Oncogenic microRNA of Squamous Cell Carcinoma of Tongue. Clin Cancer Res 14: 2588–2592.
55. Mathas S, Hinz M, Anagnostopoulos I, Krappmann D, Lietz A, et al. (2002) Aberrantly expressed c-Jun and JunB are a hallmark of Hodgkin lymphoma cells, stimulate proliferation and synergize with NF-kappa B. EMBO J 21: 4104–4113.
56. Szremska AP, Kenner L, Weisz E, Ott RG, Passegue E, et al. (2003) JunB inhibits proliferation and transformation in B-lymphoid cells. Blood 102: 4159–4165.
57. Bassig BA, Zheng T, Zhang Y, Berndt SI, Holford TR, et al. (2012) Polymorphisms in complement system genes and risk of non-Hodgkin lymphoma. Environ Mol Mutagen 53: 145–151.
58. Andoh A, Fujiyama Y, Hata K, Araki Y, Takaya H, et al. (1999) Counter-regulatory effect of sodium butyrate on tumour necrosis factor-alpha (TNF-alpha)-induced complement C3 and factor B biosynthesis in human intestinal epithelial cells. Clin Exp Immunol 118: 23–29.
59. Fischer WH, Jagels MA, Hugli TE (1999) Regulation of IL-6 synthesis in human peripheral blood mononuclear cells by C3a and C3a(desArg). J Immunol 162: 453–459.
60. Matsumoto M, Hsieh TY, Zhu N, VanArsdale T, Hwang SB, et al. (1997) Hepatitis C virus core protein interacts with the cytoplasmic tail of lymphotoxin-beta receptor. J Virol 71: 1301–1309.
61. Chen CM, You LR, Hwang LH, Lee YH (1997) Direct interaction of hepatitis C virus core protein with the cellular lymphotoxin-beta receptor modulates the signal pathway of the lymphotoxin-beta receptor. J Virol 71: 9417–9426.
62. You LR, Chen CM, Lee YH (1999) Hepatitis C virus core protein enhances NF-kappaB signal pathway triggering by lymphotoxin-beta receptor ligand and tumor necrosis factor alpha. J Virol 73: 1672–1681.
63. Simonin Y, Vegna S, Akkari L, Gregoire D, Antoine E, et al. (2013) Lymphotoxin Signaling Is Initiated by the Viral Polymerase in HCV-linked Tumorigenesis. PLoS Pathog 9: e1003234.
64. Vladareanu AM, Ciufu C, Neagu AM, Onisai M, Bumbea H, et al. (2010) The impact of hepatitis viruses on chronic lymphoproliferative disorders—preliminary results. J Med Life 3: 320–329.
65. Heyninck K, De Valck D, Vanden Berghe W, Van Criekinge W, Contreras R, et al. (1999) The zinc finger protein A20 inhibits TNF-induced NF-kappaB-dependent gene expression by interfering with an RIP- or TRAF2-mediated transactivation signal and directly binds to a novel NF-kappaB-inhibiting protein ABIN. J Cell Biol 145: 1471–1482.
66. Dondelinger Y, Aguileta MA, Goossens V, Dubuisson C, Grootjans S, et al. (2013) RIPK3 contributes to TNFR1-mediated RIPK1 kinase-dependent apoptosis in conditions of cIAP1/2 depletion or TAK1 kinase inhibition. Cell Death Differ 20: 1381–1392.
67. Cai X, Du J, Liu Y, Xia W, Liu J, et al. (2013) Identification and characterization of receptor-interacting protein 2 as a TNFR-associated factor 3 binding partner. Gene 517: 205–211.
68. Zhu Y, Lu Y, Zhang Q, Liu JJ, Li TJ, et al. (2012) MicroRNA-26a/b and their host genes cooperate to inhibit the G1/S transition by activating the pRb protein. Nucleic Acids Res 40: 4615–4625.
69. Ma YL, Zhang P, Wang F, Moyer MP, Yang JJ, et al. (2011) Human embryonic stem cells and metastatic colorectal cancer cells shared the common endogenous human microRNA-26b. J Cell Mol Med 15: 1941–1954.

70. Koh CM, Iwata T, Zheng Q, Bethel C, Yegnasubramanian S, et al. (2011) Myc enforces overexpression of EZH2 in early prostatic neoplasia via transcriptional and post-transcriptional mechanisms. Oncotarget 2: 669–683.
71. Song G, Xu G, Ji C, Shi C, Shen Y, et al. (2014) The role of microRNA-26b in human adipocyte differentiation and proliferation. Gene 533: 481–487.
72. Palumbo T, Faucz FR, Azevedo M, Xekouki P, Iliopoulos D, et al. (2013) Functional screen analysis reveals miR-26b and miR-128 as central regulators of pituitary somatomammotrophic tumor growth through activation of the PTEN-AKT pathway. Oncogene 32: 1651–1659.
73. Tsukiyama-Kohara K, Poulin F, Kohara M, DeMaria CT, Cheng A, et al. (2001) Adipose tissue reduction in mice lacking the translational inhibitor 4E-BP1. Nat Med 7: 1128–1132.

Recent Insights into Hepatitis B Virus–Host Interactions

Sayeh Ezzikouri,[1,2,3]* Makoto Ozawa,[2,3]* Michinori Kohara,[3,4] Naima Elmdaghri,[1] Soumaya Benjelloun,[1] and Kyoko Tsukiyama-Kohara[2,3]*

[1]*Virology Unit, Viral Hepatitis Laboratory, Pasteur Institute of Morocco, Casablanca, Morocco*
[2]*Transboundary Animal Diseases Centre, Joint Faculty of Veterinary Medicine, Kagoshima University, Kagoshima, Japan*
[3]*Laboratory of Animal Hygiene, Joint Faculty of Veterinary Medicine, Kagoshima University, Kagoshima, Japan*
[4]*Department of Microbiology and Cell Biology, Tokyo Metropolitan Institute of Medical Science, Tokyo, Japan*

Hepatitis B virus (HBV) poses a threat to global public health mainly because of complications of HBV-related chronic liver disease. HBV exhibits a narrow host range, replicating primarily in hepatocytes by a still poorly understood mechanism. For the generation of progeny virions, HBV depends on interactions with specific host factors through its life cycle. Revealing and characterizing these interactions are keys to identifying novel antiviral targets, and to developing specific treatment strategies for HBV patients. In this review, recent insights into the HBV–host interactions, especially on virus entry, intracellular trafficking, genome transcription and replication, budding and release, and even cellular restriction factors were reviewed. ***J. Med. Virol.***

KEY WORDS: HBV; host factors; receptors; cccDNA; replication; new target

INTRODUCTION

Hepatitis B virus (HBV) is the prototype of the family *Hepadnaviridae*, which is characterized by enveloped virions, incomplete double-stranded circular DNA genomes, a retrovirus-like replication strategy which depends on reverse transcription, and hepatotropic infection with a high species-specificity [Summers and Mason, 1982]. HBV virions are composed of a viral envelope with a diameter of about 42 nm that surrounds viral nucleocapsid [Dane et al., 1970]. The nucleocapsid harbors the DNA genome that is covalently linked to the viral polymerase (Fig. 1A) [Seeger and Mason, 2000]. The HBV genome (3.2 kb) contains four overlapping open reading frames (ORFs) (Fig. 1B) [Liang, 2009]. The surface (S) ORF encodes the envelope protein, which actually consists of three separate surface proteins: large (L), middle (M), and small (S) proteins. The polymerase (P) ORF encodes a multifunctional protein that is involved in encapsidation, initiation of minus strand DNA synthesis, reverse transcriptation, and degradation of pregenomic RNA (pgRNA). The core (C) ORF encodes both hepatitis B core antigen (HBcAg), which is a structural nucleocapsid core protein, and hepatitis B e antigen (HBeAg), which is a soluble nucleocapsid protein (Fig. 1C). The X ORF encodes hepatitis B x protein (HBx), which plays roles in signal transduction, transcriptional activation, DNA repair, and inhibition of protein degradation [Neuveut et al., 2010].

Abbreviations: APOBEC3, apolipoprotein B mRNA-editing enzyme catalytic polypeptide-like 3; cccDNA, covalently closed circular DNA; DHBV, duck hepatitis B virus; FTL, ferritin light chain; HBcAg, hepatitis B core antigen; HBeAg, hepatitis B e antigen; HBsAg, hepatitis B surface antigen; HBV, hepatitis B virus; HBx, hepatitis B x protein; HCC, hepatocellular carcinoma; miRNAs, microRNAs; MVB, multivesicular body MVB; NTCP, sodium taurocholate cotransporting polypeptide; pgRNA, pregenomic RNA; rcDNA, relaxed circular DNA; SCCA1, squamous cell carcinoma antigen 1

Grant sponsor: Ministry of Health, Labor and Welfare, Japan (H24-HepatitisB-014); Grant sponsor: Japan Society for the Promotion of Science (JSPS)

Conflict of interest: The authors who have taken part in this study declared that they do not have anything to disclose.

*Correspondence to: Sayeh Ezzikouri, Makoto Ozawa, or Kyoko Tsukiyama-Kohara, Transboundary Animal Diseases Centre, Joint Faculty of Veterinary Medicine, Kagoshima University, Kagoshima, Japan.
E-mail: sayeh.ezzikouri@pasteur.ma, mozawa@vet.kagoshima-u.ac.jp, kkohara@agri.kagoshima-u.ac.jp

Accepted 7 February 2014

DOI 10.1002/jmv.23916
Published online in Wiley Online Library (wileyonlinelibrary.com).

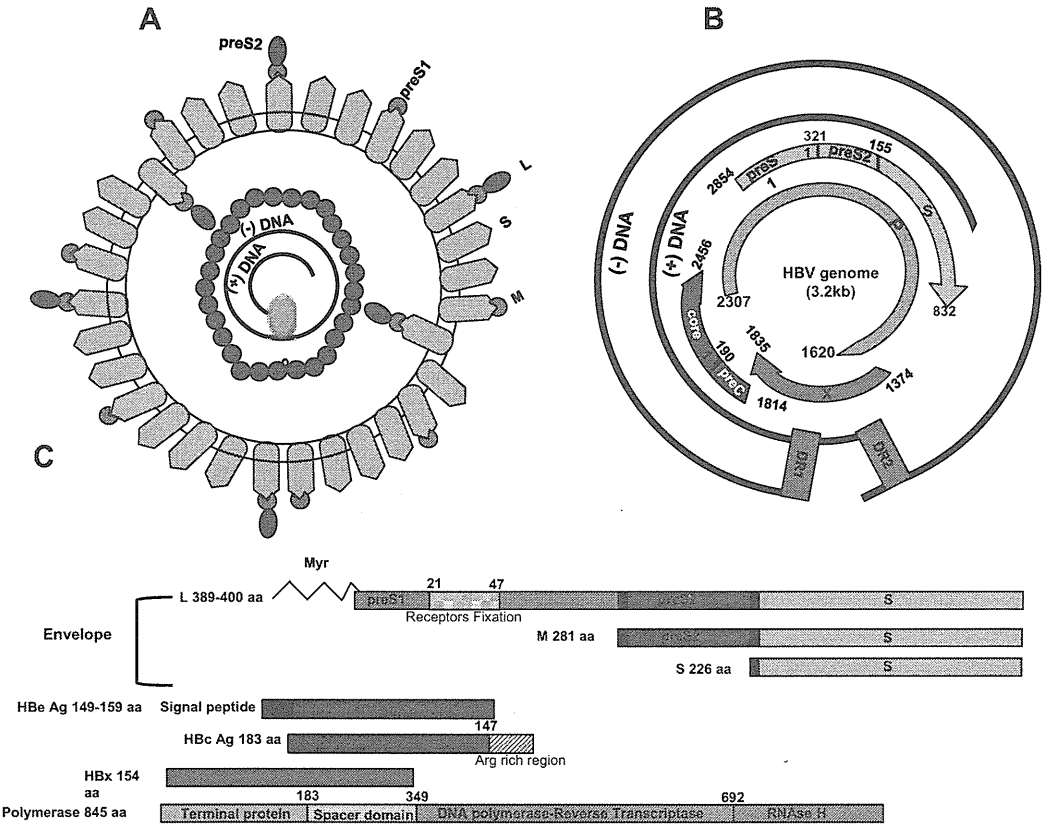

Fig. 1. Schematic structure of the HBV particle and viral proteins with domain structures. **A**: Schematic structure of HBV virion. **B**: HBV genome organization. The genome of HBV is a double-stranded DNA (3.2 kb), which contains four overlapping open reading frames (ORFs) coding for viral envelope (pre-S1/pre-S2/S), core proteins (preC/C), viral polymerase, and HBx protein (X) are shown. Two 11-bp repeats, DR1 and DR2, located at the 5′ ends of the minus and plus strands, play a critical role in viral DNA replication. **C**: Schematic representation of HBV proteins. The HBV envelope proteins consisting of L, M, and S proteins locate on the viral membrane. The L proein with 389–400 aa plays a pivotal role in receptor attachment and conatins preS1 (green), preS2 (red), and S domains (brown): the myristic acid attaches to glycine at aa position 2 of the N-terminus of preS1. The M protein with 281 aa conatins preS2 and S. The S protein encods for only the S domain (226 aa) that is crucial for virus assembly and infectivity. HBx gene is the smallest of the four partially ORF of HBV. It comprises 452 nucleotides that encode a 154-amino acid regulatory protein wich is known as a transcription factor. The precore mRNA is translated into precore protein (HBeAg), a secretory protein with 149–159 aa. The pgRNA serves as mRNAs for both viral polymerase and the core protein (183 aa) that contains an arginine rich domain (ARD) containing four stretches of clustering arginines at the C-terminus. The pgRNA subsequently functions as a template for progeny viral DNA genomes synthesized by reverse transcription. HBV polymerase protein (P, pink) with 845 aa comprises four domains: a terminal protein domain for priming of HBV replication, a spacer domain with unknown function, a reverse transcriptase (RNA-dependent DNA polymerase) domain for viral RNA transcription and replication, and an RNase H domain for degradation of pgRNA.

The clinical course of HBV infection is variable and includes acute self-limited infection, fulminant hepatic failure, an inactive carrier state, and chronic hepatitis with progression to cirrhosis and hepatocellular carcinoma (HCC) [McMahon, 2005]. Although an effective HBV vaccines is available, HBV infection is a major public health problem, and an important cause of infectious disease mortality worldwide [WHO, 2013]. Indeed, there are more than 350 million chronic carriers of HBV worldwide [Lee, 1997; Hoofnagle et al., 2007] and about 600,000 people die every year due to the complications of HBV-related chronic liver disease [WHO, 2013]. Serum hepatitis B surface antigen (HBsAg) is used as a diagnostic marker of HBV infection. Also, antibodies against HBsAg signify recovery or immunization.

Eradication of HBV infection is rendered difficult by occasional integration of covalently closed circular DNA (cccDNA) into cellular chromosomes and/or due to the unusual persistence of the episomal cccDNA in infected cell nuclei [Dejean et al., 1986]. Interferon alpha and nucleos(t)ide analogues are currently approved as antiviral agents to reduce the severity of HBV-related diseases, although these antiviral agents have limited efficacy and do not result in sustained virological response in most cases [Zoulim and Locarnini, 2009, 2012]. In addition, nucleos(t)ide analogues can result in the selection of single or even

broad antiviral-resistance mutants [Zoulim and Locarnini, 2009]. Therefore, the development of novel therapeutic strategies that interfere with other steps of the viral replication cycle and improve treatment outcomes are needed. To this end, an understanding of HBV biology and pathogenesis is important. In this review, available literatures concerning molecular mechanisms underlying HBV life cycle, especially the interactions between viral and host factors are considered.

HBV ENTRY AND INTRACELLULAR TRAFFICKING

The first step in terms of the HBV life cycle is the recognition of cellular receptor by viral envelop protein; co-receptors may also contribute to binding to the cell surface and/or to host specificity and tissue tropism (Fig. 2). The L protein plays a pivotal role in the attachment to receptors, and exhibits mixed topologies one cytoplasmically oriented (an inward topology) with as essential role in nucleocapsid envelopment, and another outward topology, displaying preS1 on the exterior of the virion envelope to mediate infection via a cell-surface receptor (or receptors) [Ostapchuk et al., 1994; Prange and Streeck, 1995; Awe et al., 2008]. In terms of viral factors required for the HBV receptor recognition, it has been demonstrated that the myristoylated preS1 domain of HBV L protein plays a key role in viral infectivity by mediating attachment to specific receptor molecule(s) [Gripon et al., 1995; Schulze et al., 2007]. Recent studies by using chemically synthesized lipopeptide fragments of the HBV L-protein showed that HBV hepatotropism is mediated through specific binding of the myristoylated N-terminal preS1-subdomain of the HBV L-protein to a hepatocyte specific receptor. Moreover, the restricted infectivity of HBV to human primates is not generally determined by the absence of this binding receptor in non-susceptible hosts, but is probably related to the lack of cofactor involved in membrane fusion [Meier et al., 2013; Schieck et al., 2013]. In addition, other studies reported that a short peptide fragment encompassing amino acids (aa) 21–47 of the preS1 domain in genotypes A, B, and C (corresponding to aa 10–36 in genotypes D, E, and G) was sufficient for HBV to bind HepG2 cells (human hepatocellular liver carcinoma cell line) [Neurath et al., 1986]. This finding is consistent with the observation that aa 3–77 of the preS1 domain are crucial for viral infectivity [Le Seyec et al., 1998; Schulze et al., 2010; Zoulim and Locarnini, 2012].

Identification of cellular receptors for HBV has received substantial attention over the years. Reliable in vitro HBV infection systems, however, have not been available for a long time. Initially, cultures of primary human hepatocytes, obtained by immediate perfusion of surgically resected liver sections, had been used to study HBV infectivity [Gripon et al., 1988]. Major problems with the use of primary human hepatocytes are their limited availability, and the heterogeneity in the quality of liver cell preparations. Against such a background, the first insight into a host factor involved in HBV entry was obtained by using duck hepatitis B virus (DHBV), which also belongs to the family *Hepadnaviridae*, as a model virus: carboxypeptidase D (gp180) was identified as a host factor that binds DHBV particles with high affinity on duck hepatocytes [Kuroki et al., 1995; Tong et al., 1995; Urban et al., 1998], although it remains uncertain whether gp180 function as a receptor for DHBV infection. Primary hepatocyte cultures from *Tupaia belangeri* were also demonstrated to be infected with HBV as efficiently as primary human hepatocytes cultures of good quality [Walter et al., 1996]. Using the primary tupaia hepatocyrtes-based in vitro system, several candidates of hepatocyte membrane receptors and co-receptors for HBV have been identified [Schulze et al., 2007; Leistner et al., 2008; Yan et al., 2012].

The recent development of a proliferating HepaRG cell line, which is a human bipotent progenitor cell line capable differentiating into two different cell phenotypes (i.e., biliary-like and hepatocyte-like cells) has been established from a liver tumor associated with chronic hepatitis C [Gripon et al., 2002]. The latter has presented new possibilities to explore HBV infection in a more specific and accurate manner. This experimental tool of human-origin can be employed for investigations addressing HBV entry (attachment, receptor interaction and viral uptake). By using this newly established in vitro system, the relevance of the initial attachment to the carbohydrate side chains of hepatocyte-associated heparan sulphate proteoglycans (HSPGs) as attachment receptors for HBV infection was reported [Schulze et al., 2007; Leistner et al., 2008]. However, because of the ubiquitous expression of heparan sulfate proteoglycans, this finding does not explain the hepatotropism of HBV. Rather, it may represent a first, non-specific step of a multistep entry process.

In 2012, very interesting data regarding the cellular receptor for HBV was presented [Yan et al., 2012]. In this study, they used a photoreactive ligand peptide derived from aa 2–47 of the preS1 domain of HBV L protein as "bait" to identify interacting proteins expressed in primary tupaia hepatocyrtes to screen for putative HBV receptor molecules. The cross-linked peptide-protein complexes were purified and subjected to mass spectrometry analysis to identify cellular proteins. Comparing the mass spectrometry results of the captured proteins with a tupaia protein datasets obtained by transcriptome, they identified sodium taurocholate cotransporting polypeptide (NTCP, also known as SLC10A1) as a hepatocyte surface molecule binding the preS1 domain. NTCP is a member of the solute carrier family 10 (SLC10), the major bile acid uptake system in human hepatocytes, and localized to the

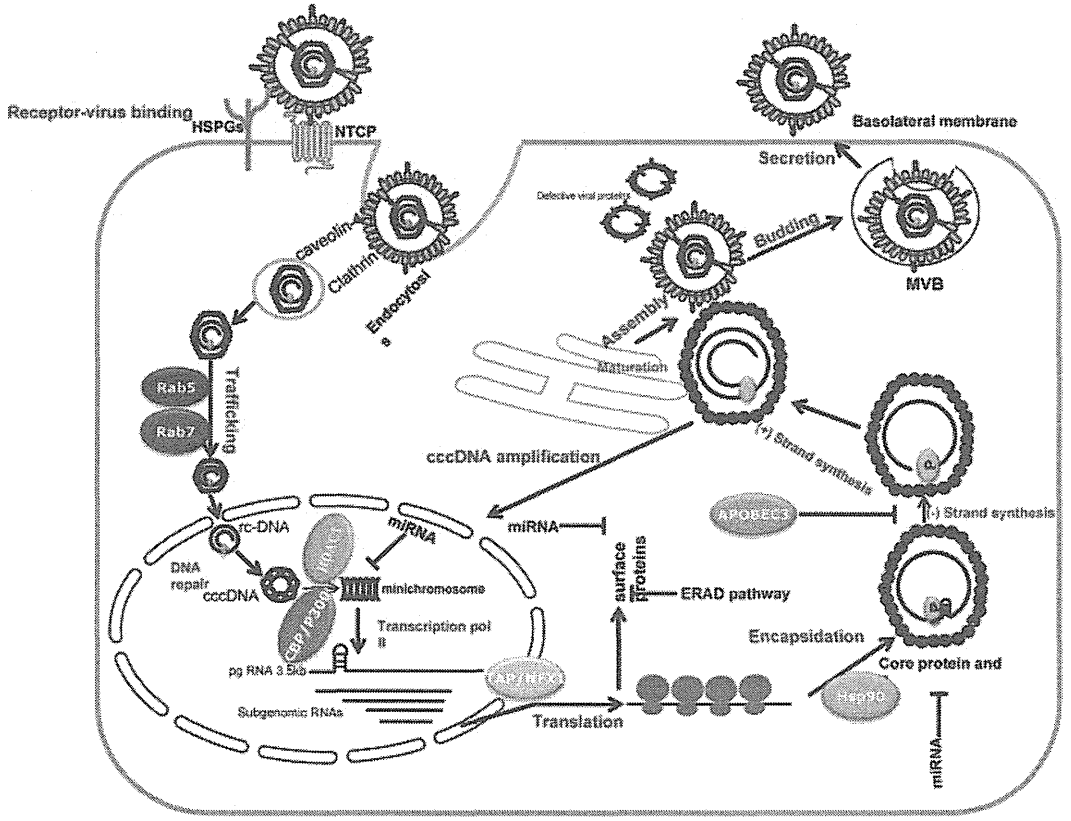

Fig. 2. Model of hepatitis B virus life cycle in polarized hepatocytes with main host factors. HBV binding receptor on hepatocytes is internalized by endocytosis and uncoated in endosome. rcDNA genome in nucleocapsid is delivered into the nucleus. The rcDNA genome, which is incomplete double-stranded circular DNA, is converted to cccDNA, which is covalently closed circular DNA by DNA repair. The cccDNA serves as a template for the viral RNA transcription mediated by the host RNA polymerase II. Viral RNAs, including the pgRNAs and subgenomic RNAs, are exported to the cytoplasm where viral RNA transcription and replication occur. The subgenomic RNAs are translated to viral proteins, the pgRNA is packaged together with polymerase protein (P) into immature nucleocapsids consisting of core proteins and reverse transcribed to the rcDNA. Mature nucleocapsids containing rcDNA are then either recycled to the nucleus to amplify the cccDNA or enveloped by the viral envelope proteins and secreted extracellularly as progeny virions. HSPGs, Heparan sulphate proteoglycans; NTCP, sodium taurocholate cotransporting polypeptide; rcDNA, relaxed circular DNA; cccDNA, covalently closed circular DNA; pgRNA, pregenomic RNA; TAP, tip-associated protein; NFX1, nuclear export factor-1, NFX ; P, HBV polymerase; Hsp 90, heat-shock protein 90; ERAD, ER-associated degradation; APOBEC3, apolipoprotein B mRNA-editing enzyme catalytic polypeptide-like 3; HDAC1, histone deacetylase 1; MVB, multivesicular body.

basolateral hepatocyte membrane [Kullak-Ublick et al., 2000]. Silencing the NTCP expression by small interfering RNAs in primary tupaia hepatocyrtes, HepaRG or primary human hepatocytes led to the reduced HBV infection. Phylogenetic analysis and mutagenesis studies showed that aa 157–165 in NTCP serve as determinants for species-specificity. Using ectopic expression of tupaia and human NTCPs in non-permissive HepG2 or HuH-7 hepatoma cells rendered these cells susceptible to HBV infection at low levels, suggesting that NTCP may not be the sole host factor supporting HBV entry. More recent data suggested that both ferritin light chain (FTL), and squamous cell carcinoma antigen 1 (SCCA1) may serve as co-receptors in HBV cellular attachment and viral entry into hepatocytes [Hao et al., 2012].

For HBV entry into cells, receptor binding is followed by endocytosis mediated by host factors. A recent in vitro study showed that a caveolin-1-mediated endocytosis is required to initiate HBV entry in HepaRG cells [Macovei et al., 2010]. In addition, disrupting the epithelial barrier of HepaRG cells was demonstrated to increase HBV infection, suggesting that the entry of HBV into hepatocytes occurs in a polarized manner, and the resulting transformation in membrane polarity renders HepaRG cells susceptible to infection by allowing access to the basolateral domain [Schulze et al., 2012].

Early reports indicated that HBV replication was cell cycle-dependent and was inversely correlated with cellular DNA synthesis: these findings may explain the elimination of virus during cell regeneration that has been observed during severe acute hepatitis B or HBV reactivation [Ozer et al., 1996]. Following endocytosis, HBV must travel through the complex network of the endocytic pathway to reach

the cell nucleus where HBV genome transcription and replication occur (Fig. 2). The intracellular trafficking events which are critical for the initiation of a productive infection by providing the appropriate environment for virus uncoating and nucleocapsid release, have remained completely obscure for HBV. Indeed, recent study showed that HBV infection strongly depends on the expression of host factors Rab5 and Rab7 [Macovei et al., 2013], both of which are GTPases involved in the endosome biogenesis [Somsel Rodman and Wandinger-Ness, 2000]. In this study, authors investigated the effect of the host factors on trafficking of HBV particles internalized in HepaRG cells by using a stable and inducible short hairpin RNA expression system. The results showed that silencing of either Rab5 or Rab7 expression results in significant inhibition of the early stages of HBV infection, indicating that HBV transport from early to mature endosomes is required for HBV life cycle.

An understanding of the HBV entry mechanism may represent a rather new and attractive therapeutic concept to combat HBV infection both in the acute and chronic phases. In fact, several studies have shown that a lipopeptide derived from the preS1 domain is a promising drug additive that can be used to improve patient treatment outcomes [Gripon et al., 2005; Petersen et al., 2008; Volz et al., 2013].

HBV GENOME TRANSCRIPTION AND REPLICATION

After fusion of viral and cellular membranes in endosomes, the capsid delivers its relaxed circular DNA (rcDNA), which is held in circular conformation by a short cohesive overlap between the 5′ ends of the two DNA strands, into the nucleus through nuclear pore complex (NPC). Passage through the NPC is mediated by the interaction between a nuclear localization signal on the C terminal of the viral capsid proteins and nuclear import receptors importin α and β [Kann et al., 1999]. Upon translocation to the nucleus, the rcDNA is converted to a cccDNA by a mechanism largely unknown and most probably involves cellular repair enzymes [Wei et al., 2010]. The minus strand DNA of the cccDNA serves as a template for transcription of both pgRNA and subgenomic RNA, of which the former in turn serves as the template for the reverse transcriptional synthesis of viral DNA, and the latter as the message for viral proteins by the host cell RNA polymerase II [Seeger and Mason, 2000]. The cccDNA also functions as an HBV reservoir responsible for persistent replication, and thus is considered to be a reliable marker for HBV infection [Levrero et al., 2009]. Viral HBx has been shown to be essential for the initiation and maintenance of transcription from HBV cccDNA: HBx stimulates the acetylation of histones associated with cccDNA, and is required for transcription in the context of HBV infections [Lucifora et al., 2011].

In a DHBV model, several cellular transcription factors, such as C/EBP, HNF1, and HNF3, have been demonstrated to bind the DHBV cccDNA enhancer region in duck liver extracts [Liu et al., 1994]. HBx has been proposed to promote HBV gene expression by recruiting the histone acetylases CBP/p300 and PCAF/GCN5 to the cccDNA [Belloni et al., 2009]. In addition, a recent study showed that HBx promotes gene expression from the natural HBV cccDNA, but not from a chromosomally integrated HBV [van Breugel et al., 2012]. It has been reported that HBV replication is regulated by the acetylation status of histones H3 and H4 bound to cccDNA minichromosome [Pollicino et al., 2006]. Furthermore, it appears that cellular acetyltransferases, p300 and CBP, and a cellular deacetylase, HDAC1, are recruited to bind the HBV cccDNA in vitro and in vivo [Belloni et al., 2009]. Recently, several studies have reported that a number of liver-enriched transcription factors and nuclear receptors, including STAT3 and HNF1/4, binds HBV promoter/enhancer elements [Wang et al., 2009], and to be critical in the regulation of HBV transcription [Quasdorff and Protzer, 2010]. Interestingly, most of these transcription factors/nuclear receptors are potential linkers between major cellular events in the hepatocyte (i.e., hepatic gluconeogenesis and lipid metabolism, etc.) and HBV life cycle [Bar-Yishay et al., 2011].

HBV pgRNA in the nucleus was demonstrated to be exported to the cytoplasm by associating with a cellular Tip-associated protein/nuclear export factor-1 (TAP/NFX1) and HBcAg [Li et al., 2010]. In the cytoplasm, the pgRNA is translated to HBV core protein and polymerase [Chang et al., 1990]. Binding of the HBV polymerase to RNA stem-loop structure epsilon of pgRNA initiates packaging of the single viral RNA molecule into immature nucleocapsids [Summers and Mason, 1982]. A recent study using DHBV showed that host chaperones Hsc70, Hsp40, Hsp90 plus ATP regulate reverse transcriptional activity of the viral polymerase [Stahl et al., 2007]. Reverse transcription of pgRNA into minus strand DNA is followed by degradation of the pgRNA by the RNAse H domain in the HBV polymerase. The degradation is complete except for its 5' terminal, 15–18 nucleotides which serve as a primer for plus-strand DNA synthesis resulting in rcDNA formation [Beck and Nassal, 2007; Nassal, 2008]. Mature capsids containing rcDNA can be either recycled for intracellular cccDNA amplification [Tuttleman et al., 1986; Locarnini and Mason, 2006], or assembled with viral surface proteins in the endoplasmic reticulum to form progeny viral particles that will be released from the cell [Ganem, 1991; Locarnini and Zoulim, 2010; Dandri and Locarnini, 2012].

HBV BUDDING AND RELEASE

HBV virions are assembled in the endoplasmic reticulum (ER)-Golgi compartment [Patient et al., 2007]

(Fig. 2). A recent report showed that HBV activates the ER-associated degradation (ERAD) pathway, which in turn, reduces the levels of HBV envelope proteins, possibly as a mechanism to control the level of viral particles in infected cells, and facilitate the establishment of chronic infections [Lazar et al., 2012]. The budding and release of HBV virions from hepatocytes have been suggested to involve the machinery of multivesicular body (MVB), including the interaction of host factors γ2-adaptin, Nedd4 ubiquitin ligase, Vps4, VPS4B, and AIP1 [Hartmann-Stuhler and Prange, 2001; Rost et al., 2006; Watanabe et al., 2007]. The molecular mechanisms underlying HBV budding and release, remain largely unknown. However, knowledge in this area has the potential to lead to a new class of therapeutic agents.

HBV RESTRICTION FACTORS

Recently, some variants of human apolipoprotein B mRNA-editing enzyme catalytic polypeptide-like 3 (APOBEC3), that is, APOBEC3B, APOBEC3C, APOBEC3F, APOBEC3G, and APOBEC3H, have been shown to affect HBV by two ways: introducing G-to-A hypermutations into the nascent minus strand DNA of HBV by their deaminase activities [Turelli et al., 2008; Henry et al., 2009; Noguchi et al., 2009; Ezzikouri et al., 2013] and by inhibiting HBV reverse transcription independent of the deaminase activities [Rosler et al., 2004; Turelli et al., 2004]. Previous studies have shown that the prevalence of hypermutated HBV genomes (G > A transitions) varies between 2% and 35% [Noguchi et al., 2009; Vartanian et al., 2010; Ezzikouri et al., 2013]. The role of these restriction factors listed above in the regulation of HBV replication needs further investigation to fully elucidate their therapeutic potential.

MicroRNAs (miRNAs) are important small noncoding RNAs that regulate post-transcriptional gene expression in diverse biological processes such as development, immune response, and tumorigenesis [Lindsay, 2008; Pedersen and David, 2008; Nana-Sinkam and Croce, 2013]. Several studies have shown that HBV replication is also regulated by several miRNAs (miR-1, miR-141, miR-449a, miR-210, miR-152, miR-148a, etc.) that lead to modification of host gene expression [Liu et al., 2011; Zhang et al., 2011; Hu et al., 2012]. In fact, miR-141 suppressed HBV replication by reducing HBV promoter activities through the down-regulation of peroxisome proliferator activated receptor alpha [Hu et al., 2012] and miR-125a-5p interferes with the HBV translation and down-regulation of the expression of the surface antigen, thus reducing the amount of secreted HBsAg [Potenza et al., 2011]. In addition, other group showed that miR-1 was able to enhance the HBV core promoter transcription activity by up-regulating of farnesoid X receptor alpha expression [Zhang et al., 2011].

More recently in chronic hepatitis B patients, the miR-122 was found to be specifically suppressed and led to enhanced HBV replication [Wang et al., 2012]. The loss of miR-122 expression by viral mRNAs and/or chronic inflammation leads to upregulation of its target binding factor, which initiates pituitary tumor transforming gene (PTTG1) nuclear translocation, promoting PTTG1 transcriptional activity and thus enhancing cell growth and invasion [Li et al., 2013]. These data provide a potential new strategy for the development of novel therapies to prevent the development of HCC under HBV infection. However, the mechanism underlying the miR-122-mediated regulation of viral mRNAs is unknown. The relationship between miRNAs and HBV infection offers a promising miRNA-based HBV therapy in the future.

CONCLUSIONS AND PERSPECTIVES

To gain insights into HBV infection, advances in molecular virology are indispensable. The studies reviewed above have significantly enhanced the understanding of some cell biological aspects of HBV–host interactions. Despite significant experimental hurdles, numerous *bona fide* HBV host interactions have been defined with the most recent data about the discovery of NTCP that allows new insight in the improvement of cell culture systems, such, HepaRG-NTCP, and HepG2-NTCP cells. These in vitro systems will be also accelerated the acquisition of data revealing the interplay between HBV and host factors and design new therapy. The most challenging goal, will be to understand the assembly, budding, and release of HBV particle and to develop a small animal model system for HBV studies, which will have strong implications for drug development and the decipher of hepatitis B pathogenesis.

ACKNOWLEDGMENTS

We are particularly grateful to Prof. George Wu for editing the manuscript. This research was supported by a grant from the Ministry of Health, Labor, and Welfare, Japan (H24-HepatitisB-014). Sayeh Ezzikouri is supported by Japan Society for the Promotion of Science (JSPS) Fellowships for Foreign Researchers. We apologize to the many HBV investigators whose work could not be cited owing to space restrictions.

REFERENCES

Awe K, Lambert C, Prange R. 2008. Mammalian BiP controls posttranslational ER translocation of the hepatitis B virus large envelope protein. FEBS Lett 582:3179–3184.

Bar-Yishay I, Shaul Y, Shlomai A. 2011. Hepatocyte metabolic signalling pathways and regulation of hepatitis B virus expression. Liver Int 31:282–290.

Beck J, Nassal M. 2007. Hepatitis B virus replication. World J Gastroenterol 13:48–64.

Belloni L, Pollicino T, De Nicola F, Guerrieri F, Raffa G, Fanciulli M, Raimondo G, Levrero M. 2009. Nuclear HBx binds the HBV minichromosome and modifies the epigenetic regulation of cccDNA function. Proc Natl Acad Sci U S A 106:19975–19979.